



## **An overview on the removal of synthetic dyes from water by electrochemical advanced oxidation processes**

P V Nidheesh, Minghua Zhou, Mehmet A. Oturan

### **► To cite this version:**

P V Nidheesh, Minghua Zhou, Mehmet A. Oturan. An overview on the removal of synthetic dyes from water by electrochemical advanced oxidation processes. *Chemosphere*, 2018, 197 (210-227.), <10.1016/j.chemosphere.2017.12.195>. <hal-01721053>

**HAL Id: hal-01721053**

**<https://hal.science/hal-01721053v1>**

Submitted on 1 Mar 2018

**HAL** is a multi-disciplinary open access archive for the deposit and dissemination of scientific research documents, whether they are published or not. The documents may come from teaching and research institutions in France or abroad, or from public or private research centers.

L'archive ouverte pluridisciplinaire **HAL**, est destinée au dépôt et à la diffusion de documents scientifiques de niveau recherche, publiés ou non, émanant des établissements d'enseignement et de recherche français ou étrangers, des laboratoires publics ou privés.



HAL Authorization

# **An overview on the removal of synthetic dyes from water by electrochemical advanced oxidation processes**

**P. V. Nidheesh<sup>1</sup>, Minghua Zhou<sup>2</sup>, Mehmet A. Oturan<sup>3,\*</sup>**

<sup>1</sup> CSIR-National Environmental Engineering Research Institute, Nagpur, Maharashtra, India

<sup>2</sup> Key Laboratory of Pollution Process and Environmental Criteria, Ministry of Education,  
Tianjin Key Laboratory of Urban Ecology Environmental Remediation and Pollution  
Control, College of Environmental Science and Engineering, Nankai University, Tianjin  
300350, P. R. China.

<sup>3</sup> Université Paris-Est, Laboratoire Géomatériaux et Environnement, (LGE), , EA 4508,  
UPEM, 5 Bd Descartes, 77454 Marne-la-Vallée Cedex 2, France

**Paper submitted for publication in SI: EAOPs-POPs, Chemosphere**

\*Corresponding author:

Email: [Mehmet.Oturan@univ-paris-est.fr](mailto:Mehmet.Oturan@univ-paris-est.fr) (Mehmet A. Oturan)

Tel.: +33 (0)1 49 32 90 65

## **Abstract**

Wastewater containing dyes are one of the major threats to our environment. Conventional methods are insufficient for the removal of these persistent organic pollutants. Recently much attention has been received for the oxidative removal of various organic pollutants by electrochemically generated hydroxyl radical. This review article aims to provide the recent trends in the field of various electrochemical advanced oxidation processes (EAOPs) used for removing dyes from water medium. The characteristics, fundamentals and recent advances in each processes namely anodic oxidation, electro-Fenton, peroxicoagulation, ferred Fenton, anodic Fenton, photoelectro-Fenton, sonoelectro-Fenton, bioelectro-Fenton etc. have been examined in detail. These processes have great potential to destroy persistent organic pollutants in aqueous medium and most of the studies reported complete removal of dyes from water. The great capacity of these processes indicates that EAOPs constitute a promising technology for the treatment of the dye contaminated effluents.

**Keywords:** Dye removal, Electrochemical advanced oxidation, Decolorization, Mineralization, Hydroxyl radicals, Wastewater treatment

## 1. Introduction

Water pollution due to various industrial effluents is a global environmental problem. Due to the rapid industrialization, the use of coloring chemicals like dyes also increases day by day. Overall, 40,000 dyes and pigments with more than 7,000 different chemical structures have been reported recently (Demirbas, 2009). Production of dyestuff and pigments annually across the world is more than 700,000 tonnes and in India itself it is close to 80,000 tonnes (Mathur et al., 2005; Gong et al., 2007; Mane et al., 2007). Among this 10,000 different types of dyes and pigments are being manufactured annually across the world (Ponnusami et al., 2008). These dyes are chemically, photolytically and biologically highly stable and are highly persistent in nature (Suteu and Bilba, 2005). Various industries like textile, leather, food, cosmetic, paper, pharmaceutical etc. are using variety of synthetic dyes. Among these industries, textile industries are the largest consumer of dying stuffs and pigments and produces large amount effluents after dyeing process. For example, 1.5 million liters per day of effluent are discharging into natural water bodies from an average mill producing  $60 \times 10^4$  m of fabric (COINDS, 2000). This wastewater contains various kinds of pollutants apart from dyes and most of them are hazardous. Depending on the textile processes, effluents generated from the industry contains various types of solvents, salts, detergents etc. apart from many types of dyes (Barredo-Damas et al., 2006). Typical characteristics of the effluent generated from textile industries are given in Table 1. Among these contaminants, removal of dyes from the wastewater needs to be a special attention.

The effluents containing dyes are one of the major threats to environment. Even in low concentrations, the dyes are highly visible (esthetic pollution) and affect the aquatic life and food chain (chemical pollution) (Namasivayam and Kavitha, 2002; Malik, 2003). However, the average concentration of dyes in a textile wastewater is around  $300 \text{ mg L}^{-1}$  (Couto, 2009). Disposal of this highly colored wastewater into natural water bodies hamper light penetration,

distress biological process in the water medium and provide an aesthetically displeasing appearance (Arivoli et al., 2009). Reduced light penetration with the introduction of colored wastewater reduces the photosynthetic activity within the water body and this also affect the symbiotic process (Ju et al., 2008).

**Table 1** Characteristics of textile wastewater. Reprinted with permission from Sandya et al. (2008), Copyright 2007, Elsevier.

Parameters	Concentration
Solution pH	9.5-12.5
Total Suspended Solids (mg L <sup>-1</sup> )	60-416
Total Dissolved Solids (mg L <sup>-1</sup> )	4500-12800
Total Organic Carbon (mg L <sup>-1</sup> )	26390-73190
Biochemical Oxygen Demand (mg L <sup>-1</sup> )	25-433
Chemical Oxygen Demand (mg L <sup>-1</sup> )	1835-3828
Aromatic Amines (mg L <sup>-1</sup> )	20-75
Ammonia (mg L <sup>-1</sup> )	2-3
Chloride (mg L <sup>-1</sup> )	1200-1375
Sulphate (mg L <sup>-1</sup> )	700-2400

The hazardous, toxic and carcinogenic natures of dyes are also well known. Physiological disorders in aquatic organisms happen by the consumption of dyes in textile effluents via food chain (Karthikeyan et al., 2006). Some of the azo dyes are responsible for causing bladder cancer in humans and chromosomal aberration in mammalian cells (Mendevedev, 1988; Percy et. al., 1989). Cytotoxicity of reactive dyes (three monochlortriazinyl dyes: yellow, red and blue with different concentrations) using human keratinocyte HaCaT cells in vitro was investigated by Klemola et al. (2007) and the mean inhibitory concentration values after 72 h of exposure was measured as 237 µg mL<sup>-1</sup> for yellow dye, 155 µg mL<sup>-1</sup> for red dye and 278 µg mL<sup>-1</sup> for blue dye. Similarly, spermatozoa

motility inhibition test of these dyes showed the mean inhibitory concentration values after 24 h of exposure as  $135 \mu\text{g mL}^{-1}$  for yellow dye,  $\mu\text{g mL}^{-1}$  for red dye and  $127 \mu\text{g mL}^{-1}$  for blue dye (Klemola et al., 2006). Frame-shift mutation and base pair substitution in Salmonella in the presence of CI disperse blue was observed by Umbuzeiro et al. (2005). Experimental investigations of Bae and Freeman (2007) reported that C.I. Direct Blue 218 is very toxic to daphnids. The 50% of mortality of daphnids was observed for concentrations of  $1\text{-}10 \text{ mg L}^{-1}$  of C.I. Direct Blue 218 after 48 h. Impact of textile effluents on a proteinous edible fresh water fish Mastacembelus Armatus was examined by Karthikeyan et al. (2006) and they observed a decrease in  $\text{Na}^+$  and  $\text{Cl}^-$  concentrations and increase in  $\text{K}^+$ ,  $\text{Mg}^{2+}$  and  $\text{Ca}^{2+}$  concentrations after 35 d of Acid Blue 92 exposure. The toxicity of the textile dye industry effluent on freshwater female crab, Spiralothelphusa hydrodroma was investigated by Sekar et al. (2009). The authors observed a decrease in protein, carbohydrate and lipid contents in ovary, spermatheca, muscle, hepatopancreas, gill, brain, thoracic ganglia and eyestalks at 30 d of sublethal (69.66 ppm) concentration of textile dye industry effluent exposure. Mathur et al. (2005) tested the mutagenic activity of seven dyes by Ames assay, using strain TA 100 of Salmonella typhimurium and reported that except violet dye, all are mutagenic. Among these mutagenic dyes, Congo red and royal blue dyes are moderately mutagenic while bordeaux is highly mutagenic or extremely mutagenic. Similarly, effect of malachite green on immune and reproductive systems was observed by Srivastava et al. (2004). The authors also observed the potential genotoxic and carcinogenic nature of the mentioned basic dye.

These non-exhaustive examples highlight how much the presence of the dyes in water is harmful to the aquatic environment. Therefore, removal of dyes from aqueous medium is an important environmental issue in the environmental safety point of view.

84

## 85   **2. Electrochemical advanced oxidation processes for dye removal**

86       Various treatment techniques such as adsorption, coagulation, filtration,  
87   electrocoagulation, photolysis, sonolysis, biodegradation, wet land treatment, ozonation,  
88   photocatalysis, membrane filtration etc. have been used for removing synthetic dyes from  
89   aqueous solution. Advantages and disadvantages of dye removal methods have been  
90   discussed in detail ([Crini, 2006](#); [Martinez-Huitle and Brillas, 2009](#); [Nidheesh et al., 2013](#)).  
91   Based on the principle mechanism behind the removal of dyes, these processes can be  
92   divided into two broad classes: Separative (physical, and physicochemical) methods, and  
93   degradative (chemical and biological) methods. The schematic diagram of the various  
94   methods used for the dye removal is shown in [Fig. 1](#). Most of the methods used for dye  
95   removal are separation process and the main disadvantage of these processes is the disposal  
96   of dye containing sludge as in coagulation process, dye sorbed adsorbents and concentrated  
97   dye solution as in membrane processes. In contrary to this, complex dye compounds undergo  
98   a series of degradation in chemical degradation methods. In the case of use of advanced  
99   oxidation processes, degradation procedure advance until ultimate oxidation degree, i.e.  
100   mineralization of organic pollutants. These methods produce carbon dioxide, water and  
101   various inorganic ions (following heteroatoms presents at the starting organic pollutants) as  
102   the final products.

103

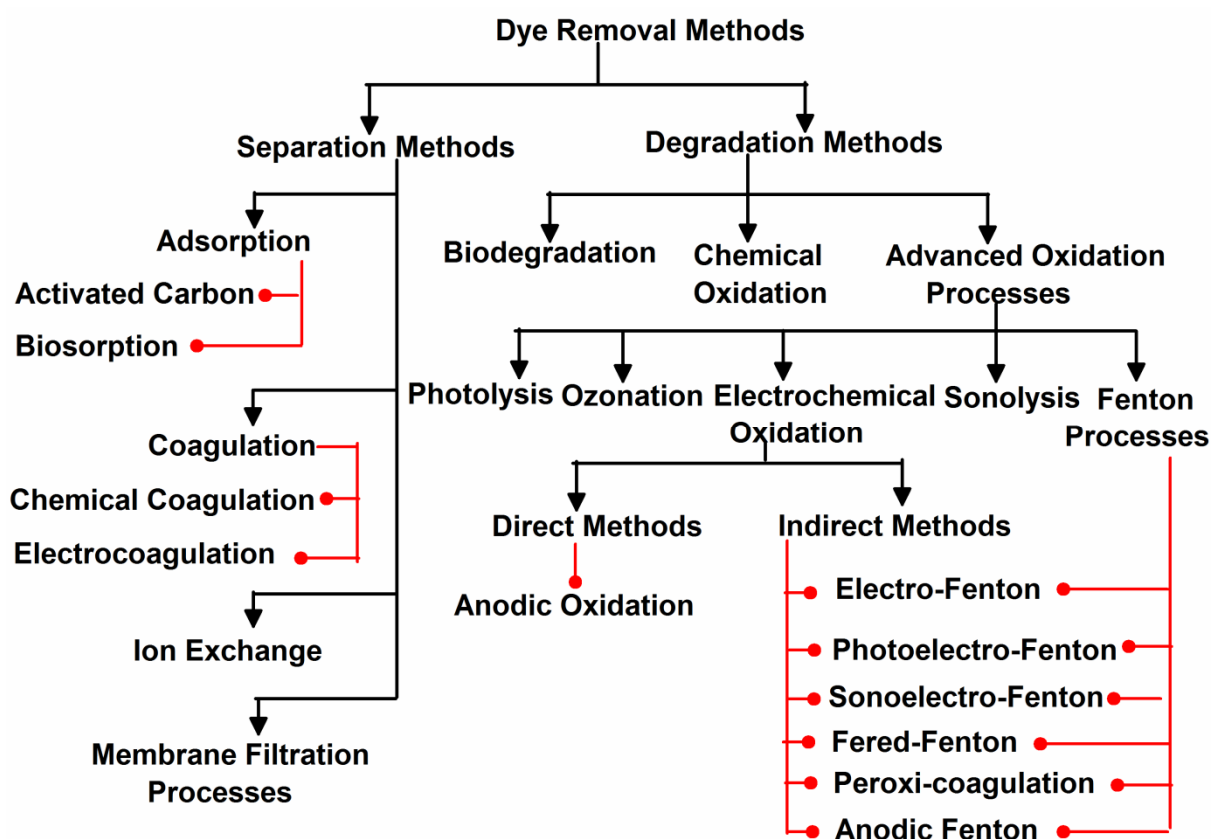


**Fig. 1** Schematic representation of method used in dye removal from water

Among various degradation techniques, advanced oxidation processes (AOPs) received great attention for the efficient degradation of dyes, during recent years (Martinez-Huitle et al., 2009, Oturan and Aaron, 2014). These processes are based on the production of highly reactive oxidants, mainly hydroxyl radical ( $\cdot\text{OH}$ ). This radical is the second most powerful oxidizing agent (after fluorine) with a redox potential of  $E^\circ (\cdot\text{OH}/\text{H}_2\text{O}) = 2.8 \text{ V/SHE}$ . Once these radicals are produced in situ, they attack organic pollutants with high reaction rates through following three different ways (Oturan, 2000; Brillas et al., 2009; Sirés et al., 2014): electron transfer (redox reaction) (Eq. (1)), H atom abstraction (dehydrogenation) (Eq. (2)), and electrophilic addition to  $\pi$  systems (hydroxylation) (Eq. (3)). These reactions produce organic radicals and start a radical chain including reactions with oxygen (formation of peroxy radicals) and formed reaction intermediates undergo further oxidation reactions with

generated oxidizing agents ( $\cdot\text{OH}$ ,  $\text{HO}_2\cdot$ ,  $\text{H}_2\text{O}_2\ldots$ ) until the complete mineralization of organic pollutants.



Among the AOPs, electrochemical advanced oxidation processes (EAOPs) that have been developed during the last decade have generated great interest for the abatement of various persistent organic pollutants including synthetic dyes. EAOPs use electrolytically produced hydroxyl radicals for the mineralization of organic pollutants. Based on the production of hydroxyl radicals in the electrolytic system, EAOPs can be divided into two categories: direct and indirect EAOPs as shown in Fig. 1. In the case of direct EAOPs, hydroxyl radicals are produced on the anode surface by direct oxidation of water according to the Eq. (4):



with M: anode material. The production rate and extent depend on the nature (catalytic activity) of anode material, diffusion rate of organic pollutants on the active sites of anode and applied current density (Panizza and Cerisola 2009; Miled et al., 2010). The great advantage of this process is to not require the external addition of reagents for the production of hydroxyl radicals. In the case of indirect EAOPs, the generation of hydroxyl radicals is based on the Fenton chemistry including *in situ* electrochemical generation (electro-Fenton) or externally addition of the one of the reagent ( $\text{H}_2\text{O}_2$  or ferrous iron) (fered-Fenton). Mostly  $\text{H}_2\text{O}_2$  is *in situ* produced at the cathode thanks to the use of an adequate electrode material. Hydroxyl radicals are produced by the reaction between electrolytically generated or externally added  $\text{H}_2\text{O}_2$  and anodically generated or externally added ferrous iron (Brillas et

al., 2009). Electro Fenton process constitutes an excellent example of indirect EAOPs, in which hydroxyl radicals are produced by the reaction between electrochemically *in situ* generated H<sub>2</sub>O<sub>2</sub> and electrocatalytically regenerated ferrous ion.

EAOPs have several advantages over conventional treatment techniques. The main advantage of the EAOPs is environmental compatibility as the main reagent for all the EAOPs is electron, which is an inbuilt clean species (Peralta-Hernández et al., 2009). Other advantages are related to their versatile nature, higher pollutant removal efficiency, operational safety and amenability of automation (Jüttner et al., 2000; Anglada et al., 2009, Sirés et al., 2014). In addition, the presence of salt (e.g., NaCl) in wastewater could help to improve process efficiency and reduce energy consumption (Zhou et al., 2011a, 2011b).

The main aim of this review is to present a general review on the application of EAOPs for the removal of dyes from aqueous solution. Special attention is made on fundamental reactions involved of each EAOP to provide clear idea on its characteristics and oxidation capacity.

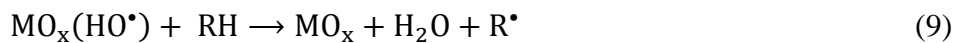
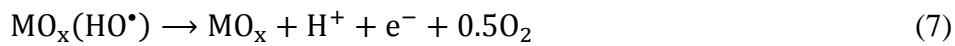
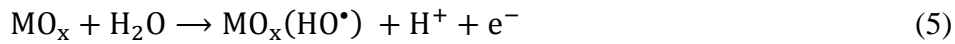
### 3. Direct EAOPs

Direct EAOPs produces hydroxyl radicals in the electrochemical reactor without the external addition of chemicals. Anodic oxidation (called also electrooxidation) is the best example of direct EAOPs. The following section explains the recent trends in dye removal by anodic oxidation process.

#### 3.1 Anodic Oxidation

Anodic oxidation (AO) is the most popular direct EAOPs; it works based on the hydroxyl radical production at the anode surface (Panizza and Cerisola, 2009). The process is heterogeneous and hydroxyl radicals formed are adsorbed on the anode surface. They are

chemisorbed in the case of active anode like Pt or DSA and are less available. The production of hydroxyl radicals is promoted by high O<sub>2</sub> evolution overvoltage anodes such as boron-doped diamond (BDD) thin film anodes. In these latter cases, hydroxyl radicals are physisorbed and consequently more available for oxidation of organics. Various researchers well explained the organic pollutant degradation mechanism in AO process in the case of metal oxide (MO<sub>x</sub>) anodes (Comninellis, 1994; Scialdone, 2009). Heterogeneous hydroxyl radicals MO<sub>x</sub>(HO•) are mainly formed by the oxidation of water (Eq. (5)). The adsorbed radicals result in the production of chemisorbed oxygen (Eq. (6)) or oxygen evolution (Eq. (7)). The chemisorbed oxygen also undergoes further reaction and produces oxygen as in Eq. (8). The MO<sub>x</sub>(HO•) and oxygen oxidize the organic pollutant as in Eqs. (9) and (10). The surface of the anode is catalytically regenerated according to Eqs. (7)-(10).



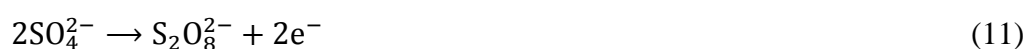
There are two ways of pollutant degradation mechanism in AO process (Comninellis and Battisti, 1996): electrochemical conversion: degradation of persistent organic pollutants into biodegradable byproducts such as short-chain carboxylic acids, and electrochemical combustion or incineration (complete mineralization of organic pollutants into CO<sub>2</sub>, H<sub>2</sub>O and inorganic ions). Between the oxidants produced in AO electrolytic cell, MO<sub>x</sub>(HO•) causes the complete mineralization of the organic pollutants and the chemisorbed oxygen (MO<sub>x</sub>(HO•)) causes the selective oxidation of organic pollutants (Chen, 2004). This

189 difference in the oxidation ability of these two oxidants is mainly due to their different  
190 oxidation potentials. Overall, AO process can be defined as the direct EAOPs in which the  
191 degradation of the organic pollutants occurs mainly by the adsorbed hydroxyl radicals  
192 produced by the water oxidation in the presence of high O<sub>2</sub> overvoltage anodes.

193 Compared with other treatment processes, AO process has several advantages. The  
194 major three advantages of AO process are (Chen et al., 2003): rapid degradation of pollutants,  
195 elevated removal efficiency, and easy operation. Apart from this, high efficiency at various  
196 solution pH is also promotes the practical implementation of AO process. In general hydroxyl  
197 radical formation is better in acidic media but the difference is not significant. Thus it was  
198 reported that heterogeneous hydroxyl radicals are also formed at pH  $\geq 10$  (Sirés et al., 2006;  
199 Özcan et al., 2008a). Even though complete mineralization of clofibric acid (Sirés et al.,  
200 2006) and 4,6-dinitro-o-cresol (Flox et al., 2005) at pH 12 was reported.

201 In AO, selection of anode affects significantly the efficiency of the process. There are  
202 two types of anodes in AO process: active and non-active anodes. This differentiation is  
203 mainly based on the reaction of anode material with adsorbed hydroxyl radicals. In the case  
204 of active anodes, formation of higher oxides or super oxides occurs by the reaction of anode  
205 with hydroxyl radicals. This reaction happens when the anode has higher oxidation potential  
206 above the standard potential required for the oxygen evolution (Migliorini et al., 2011). The  
207 anodes like Pt, IrO<sub>2</sub>, SnO<sub>2</sub> and RuO<sub>2</sub> are the examples of active anodes. On the other hand,  
208 hydroxyl radicals are physically sorbed on the non-active anodes and the mineralization of  
209 organic pollutants occurs mainly by the direct reaction of physisorbed hydroxyl radicals.  
210 These electrodes do not contribute any direct anodic reaction of organic pollutants and do not  
211 impart any catalytic site for the effective pollutant sorption (Migliorini et al., 2011). BDD  
212 electrode is the best example of non-active anodes.

Compared to active electrodes, non-active electrodes have high mineralization capacity. For example, BDD anode was found to be the best electrode for the mineralization of various persistent organic pollutants. This is mainly due to its greater O<sub>2</sub> overvoltage (which increases the hydroxyl radical production rate), its wide potential window, low background current and very low activity for O<sub>2</sub> evolution reaction (Braga et al., 2010; Migliorini et al., 2011; Oturan et al., 2012; Haidar et al., 2013). The removal of adsorbed organics on the BDD surface is also easy. In most of the cases, rinsing with appropriate solvent is required for the effective cleaning of BDD surface (Migliorini et al., 2011). The degradation of carboxylic acids by Pt is also very difficult. But the degradation of these acids is feasible with BDD anode, thanks to the efficiency of BDD(<sup>•</sup>OH) and also the strong oxidants such as peroxodisulfate and O<sub>3</sub> formed during oxidation process according to the following reactions (Muruganathan et al., 2007; Flox et al., 2009; Li et al., 2010a).



Recently a great attention has been paid to improve the efficiency of anodes by using appropriate substrate (Wang et al., 2013; Hu et al., 2014). The selection of suitable substrate is also an important parameter. A substrate should have good electrical conductivity, sufficient mechanical strength, and electrochemical inertness or easy formation of protective films on substrate surfaces by passivation (Chen et al., 2003). For example, various substrates like Si, Ti, Nb etc. were used as substrate for BDD anode. The substrate used for the BDD anode has been classically Si. But, Si is difficult to use as a substrate for electrode due to its fragile nature and its conductivity is strongly dependent on the experimental environments (Sun et al., 2011). Among the various substrates, the suitable substrate for the BDD anode

was found as Ti (Chen et al., 2003; Sun et al., 2011). Also, the O<sub>2</sub> overvoltage potential of Ti/BDD is higher than that of Si/BDD anode (Chen, 2004).

Dye removal from aqueous solution using the AO process has been studied by various researchers. Faouzi et al. (2007) reported a total degradation and mineralization of alizarin red S by AO process using BDD anode. Similarly, complete mineralization of methyl orange in the presence of *in situ* microwave activated Pt was observed by Zhao et al. (2009). Color and COD removals from real textile effluents using BDD anode was studied by Martínez-Huitle et al. (2012) and they observed an effective reduction in color and COD after 15 h of electrolysis. Yavuz and Shahbazi (2012) used bipolar trickle tower reactor containing BDD anode for the removal of reactive black 5 in a continuous flow mode operation and achieved 97% color, ~51% COD and 29.3% TOC removal at the optimal conditions, along with the reduction in toxicity. The oxidation of methyl orange using BDD anode in a 3 L capacity electrolytic cell was studied by Ramírez et al. (2013) and obtained a 94% decolorization and 63.3% TOC removal efficiencies at the optimal conditions. Complete color and COD removals from an aqueous solution containing methylene blue in the presence of BDD anode was observed by Panizza et al. (2007). Degradation of three azoic dyes, Congo red, methyl orange, and eriochrome black T, using conductive-diamond anodes was investigated by Canizares et al. (2006) and concluded that the efficiency of the system depends only on the initial concentration of dye.

Nava et al. (2008) compared the color and COD removal efficiencies of various electrode materials for the abatement of alphazurine A dye and observed almost complete mineralization of dye with Pb/PbO<sub>2</sub> and Si/BDD electrodes, while Ti/IrO<sub>2</sub> disfavored such process. Similarly complete removal of color and COD induced by the alphazurine A using BDD anode was observed by Bensalah et al. (2009). Aquino et al. (2013) used Si/BDD anode for the degradation of reactive red 141 in a filter-press flow cell and applied response surface

methodology to determine the effects of different operating parameters on color, COD and TOC removals. The performances of Ti-Pt/ $\beta$ -PbO<sub>2</sub> and BDD anodes on the removal of reactive orange 16 in a filter press reactor were investigated by [Andrade et al. \(2009\)](#). The study concluded that even though complete dye removal is achieved by both the electrodes, BDD provided better results than Ti-Pt/ $\beta$ -PbO<sub>2</sub> due to less energy consumption. [Abdessamad et al. \(2013\)](#) compared the efficiency of monopolar and bipolar BDD electrodes for the removal of alizarin blue black B and concluded that the dye degradation efficiency of bipolar AO system is 1.2 times higher than that of monopolar AO system. [Chen et al. \(2003\)](#) were found that dye removal efficiency of Ti/BDD anode was higher than that of Ti/Sb<sub>2</sub>O<sub>5</sub>-SnO<sub>2</sub> anode. Also, Ti/BDD anode has higher dye removal efficiency in the cases of alizarin red S ([Sun et al., 2011](#)), orange II and reactive red HE-3B ([Chen et al., 2003](#)). The dye removal efficiencies of BDD and PbO<sub>2</sub> electrodes were compared by [Panizza and Cerisola \(2008\)](#) and observed a higher oxidation rate and higher current efficiency in the case of BDD anode than that of PbO<sub>2</sub> anode. At the same time, methyl orange degradation efficiency of TiRuSnO<sub>2</sub> is very much less than that of BDD and PbO<sub>2</sub> anode ([Labiadh et al., 2016](#)). Partial removal of the dye was achieved by using TiRuSnO<sub>2</sub> anode, but complete dye removal was also observed with other anodes. Even though, both anodes are efficient for the complete dye removal, complete mineralization was occurred only in the presence of BDD anode.

[Yao et al. \(2013\)](#) prepared PbO<sub>2</sub>-ZrO<sub>2</sub> nanocomposite electrodes by pulse electrodeposition and used it for the removal of methylene blue. The authors observed a 100% dye and 72.7% COD removal after 120 min of electrolysis. Similarly, [An et al. \(2012\)](#) synthesized TiO<sub>2</sub>-NTs/Sb-SnO<sub>2</sub>/PbO<sub>2</sub> anode for the abatement of C.I. reactive blue 194 and reported that the prepared electrode has a high decolorization and mineralization ability. Recent study by [do Vale-Júnior et al. \(2016\)](#) demonstrates that Sn-Cu-Sb alloy anode prepared by cold gas spray is very efficient for the degradation of dyes from water medium.

The authors observed complete acid blue-29 removal and mineralization after 300 min and 600 min of electrolysis, respectively.

Effect of boron doping in BDD anode on dye removal was investigated by [Migliorini et al. \(2011\)](#) and reported that highly boron doped electrodes has the higher reactive orange 16 removal efficiency. Similar result has been observed by [Bogdanowicz et al. \(2013\)](#).

[Rodriguez et al. \(2009\)](#) observed two different oxidation mechanisms for acid yellow 1 in the presence of BDD anodes. The oxidation of dye depends more on its initial concentration. At the lower dye concentration, the oxidation process followed pseudo first order kinetics and under the control of mass transport. While, at the higher dye concentrations, the degradation of acid yellow 1 followed zero order kinetics and reaction kinetics was controlled by charge transfer.

[Panizza and Cerisola \(2008\)](#) observed the pH independent methyl red oxidation in the range of 3 to 7. Similarly, insignificant effect of initial solution pH on dye removal by AO process using  $\text{Ti/SnO}_2\text{-Sb/PbO}_2$  was observed by [Song et al. \(2010\)](#). Similar result has been reported by [Petrucchi and Montanaro \(2011\)](#). The authors observed that even though the color removal was affected by the change in pH, the mineralization ability of BDD anode was not altered with the solution pH.

Supporting electrolyte also plays an important role on the dye removal mechanism. [Aquino et al. \(2012\)](#) studied the effects of the salt (supporting electrolyte) addition for the removal of acid blue 62, reactive red 141, direct black 22, and disperse orange 29 using conductive-diamond anodes. The authors observed a mediated electrooxidation of dyes in the presence of chloride addition. At the same time, the removal of dyes by the addition of sulphate as supporting electrolyte is mainly by the attack of hydroxyl radicals, generated from BDD anode. [Zhou et al. \(2011a\)](#) compared the methyl orange degradation by electrochemical

oxidation using BDD and mixed metal oxide anodes and found enhanced dye removal in the presence of NaCl, which is mainly attributed to the co-action of mediated oxidation from active chlorine species.

The functional groups presents in the dyes also affects the efficiency of the electrolytic system. [Saez et al. \(2007\)](#) compared the alizarin red and eriochrome black T removals in the presence of BDD anode. The authors reported two different oxidation mechanisms for dye removals, even though complete COD and color removals from both dye wastewaters were observed. The removal of alizarin red was mainly due to hydroxyl radical mediated oxidation and controlled by mass transfer process, while the removal of eriochrome black T was mainly due to electrolytically generated reagents like peroxodisulphate.

#### **4. Indirect EAOPs**

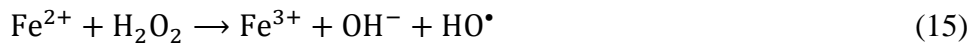
Production of hydroxyl radicals in indirect EAOPs is accomplished by the in situ production or external addition of chemicals. Fenton based EAOPs are the best examples of indirect EAOPs. The following sections discuss the applications and recent advances in these processes for the removal of dyes from aqueous medium.

##### **4.1 Electro-Fenton (EF) process**

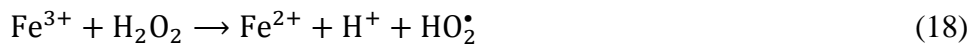
During the last decade EF process received much attraction among other processes. This is an economically and environmentally friendly process to remove efficiently toxic and/or persistent organic pollutants from water. Oturan and Brillas groups reported the principles of the EF process in the starting of 2000 ([Oturan and Pinson 1995](#); [Brillas et al., 1996](#); [Oturan, 2000](#); [Brillas et al., 2000](#)). EF process is an attractive tool and its interest is mainly due to its high degrading effectiveness of persistent organic pollutants, fast pollutant

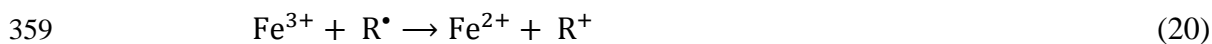
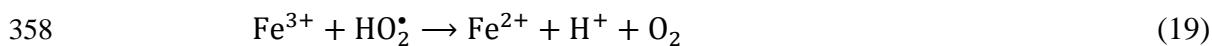
removal rate and environmental compatibility (Oturán et al., 2000; Brillas et al., 2009; Nidheesh et al., 2013; Sirés et al., 2014; Vasudevan and Oturan 2014).

EF process works based on the *in situ* electrogeneration of Fenton's reagent, a mixture of H<sub>2</sub>O<sub>2</sub> and Fe<sup>2+</sup> which is the origin of the Fenton's reaction (Eq. (15)) to generate hydroxyl radicals. Hydrogen peroxide is generated continuously at the cathode surface from the two electron reduction of O<sub>2</sub> in the acidic medium (Eq. (14)) (Oturán et al., 2008a; Özcan et al., 2009a; Nidheesh and Gandhimathi, 2012). Supply of oxygen near the cathode during EF treatment is required for fulfilling the continuous production of hydrogen peroxide in the electrolytic system. The addition of a catalytic amount of a ferrous salt (to produce Fe<sup>2+</sup> ions) into the solution leads to production of •OH according to Fenton's reaction (Eq. (15)).



Catalysis of the Fenton's reaction by electrochemical regeneration of ferrous ion is an important advantage of EF process compared to conventional Fenton process (Oturán et al., 2011; Moreira et al., 2013). Indeed, the optimal pH value for Fenton's reaction and Fenton related processes is about 3 (Brillas et al., 2009). At this pH, the predominant species of iron is Fe(OH)<sup>2+</sup> (Eq. 16) (Özcan et al., 2013). The Fe<sup>3+</sup> produced by Fenton's reaction remains under the form of Fe(OH)<sup>2+</sup> and undergoes cathodic reduction to produce ferrous ion according to Eq. (17) (Özcan et al., 2008b). Apart from this main source, ferrous ions are regenerated in the EF process via Fenton's chain reactions as in Eqs. (18-20) (Oturán et al., 2004; Oturan et al., 2010a).





where  $\text{R}^\bullet$  is organic radical.

Also, in overall, EF process results the production of two moles of hydroxyl radicals from 0.5 moles of oxygen as in Eq. (21) (Oturan et al., 2001) showing the catalytic behavior of the process.



An insignificant change in solution pH with electrolysis time is the other advantage of EF process. This is mainly due to the counterbalancing of proton consumed during the Fenton reaction by the protons produced via water oxidation at the anode (El-Desoky et al., 2010) and carboxylic acids generated during the oxidation process (Oturan and Aaron, 2014).

Carbonaceous materials are widely used as the cathode, which is the working electrode of EF process. This is mainly due to its wide range of electrochemical activity for  $\text{O}_2$  reduction and low catalytic activity for  $\text{H}_2\text{O}_2$  decomposition (Panizza and Cerisola, 2001). Also, the porosity of carbonaceous material is very high, in particular 3D carbon materials like carbon felt or graphite felt are of high porosity. These pores are useful for the sorption of oxygen gas supplied near the cathode surface and consequently results in higher amount of hydrogen peroxide generation. Various carbonaceous materials like carbon-felt (Oturan, 2000; Murati et al., 2012), reticulated vitreous carbon sheet (El-Desoky et al., 2010; Ghoneim et al., 2011), activated carbon fiber (Wang et al., 2010), graphite (George et al., 2013, 2016; Nidheesh et al., 2014a), commercial graphite-felt (Khataee et al., 2009; Panizza and Oturan, 2011) and chemically or electrochemically modified graphite felt (Zhou et al., 2013; 2014), carbon sponge (Özcan et al., 2008c) etc. were used as the cathode material for the efficient electrogeneration of hydrogen peroxide in EF cell. Özcan et al. (2008c) compared the dye

degradation efficiency of carbon sponge and carbon-felt for the abatement of acidified basic blue 3 solutions and found that carbon sponge is the effective cathode than carbon felt for EF process. By analyzing the reported literatures, various forms of Pt have been used frequently as anode in EF cell for the degradation of various organic pollutants (Nidheesh and Gandhimathi, 2012; Sopaj et al., 2015, 2016).

The efficiency of EF process increases by combining AO and EF processes. This can be achieved by the use of an O<sub>2</sub> overvoltage anode in the EF process along with the carbonaceous cathode. Oturan et al. (2012) showed that this process was able to mineralize quasi-completely the herbicide atrazine and its by-product cyanuric acid which already reported many times to be recalcitrant to hydroxyl radicals.

EF process has been proved as an efficient tool for the abatement of dyes from water medium. Nidheesh and Gandhimathi (2014a) used graphite-graphite electrolytic system for the abatement of rhodamine B (RhB) at pH 3. The authors reported that with the increase in electrode immersion depth the efficiency of the electrolytic system also increases. This is mainly due to the increased contact between cathode surface and air bubbles and the authors recommended to use bubble column reactor with lengthy electrode for the efficient removal of organic pollutants. Similarly, complete destruction of azure B and 95% TOC abatement at the end of 8 h EF treatment was observed by Olvera-Vargas et al. (2014). Almomani and Baranova (2013) analyzed the dye removal efficiencies of single and two compartment cells in the presence of stainless steel cathode and BDD anode and observed that two compartment cell is better than single cell for the removal of dyes from aqueous medium. Lakhimi et al. (2007) investigated the depollution of methylene blue, Congo red and yellow drimaren using carbon felt cathode and Pt sheet anode and observed a rapid degradation of dyes in their single and mixture solution. Almost complete mineralization of dyes also observed by Guivarch et al. (2003) and Guivarch and Oturan (2004). Similarly, 95% of the initial TOC

caused by alizarin red (Panizza and Oturan, 2011) and acid red 97 (Kayan et al., 2010) was removed effectively using the graphite-felt and carbon-felt cathodes, respectively. Diagne et al. (2014) compared the efficiencies of AO and EF processes for the removal of indigo dye and observed higher mineralization efficiency for EF process. Complete mineralization of the dye was observed within 2 h of electrolysis. Yu et al. (2015) modified graphite felt by using carbon black and PTFE; and observed 10.7 times higher  $\text{H}_2\text{O}_2$  production compared to unmodified electrode. EF process using this modified graphite felt cathode is efficient for complete removal of  $50 \text{ mg L}^{-1}$  methyl orange within 15 min and 95.7% TOC removal at 2 h electrolysis; this efficiencies being more than 4 times that of EF process operated with raw graphite felt cathode.

Apart from, solution pH, catalyst dosage, initial pollutant concentration, electrode area, applied current and inner electrode spacing; the hardness in the water also affects the efficiency of EF process significantly (dos Santos et al., 2016). The presence of magnesium and calcium in water medium reduced the dye removal efficiency of EF process for the dye eriochrome black T. This reduction in the performance of EF process is mainly related to the difficulty to break the divalent cation- eriochrome black T complex by  $\cdot\text{OH}$ .

Xu et al. (2014) prepared graphene doped gas diffusion electrode using modified Hummers' method and used for the removal of reactive brilliant blue in a three electrode undivided cell of volume 200 mL. The study concluded that under the optimal conditions, 80% of the dye and 33% of TOC were removed after 180 min of electrolysis by the novel electrode. Ghoneim et al. (2011) observed a complete dye removal and 97% of mineralization by EF process in an electrolytic cell of 600 mL capacity containing reticulated vitreous carbon cathode, platinum gauze anode and 0.2 mM sunset yellow FCF azo dye. Sirés et al. (2008) compared the dye removal efficiency of EF cell with carbon-felt cathode for the degradation of crystal violet (CV), fast green FCF (FCF), methyl green (MeG) and malachite

green (MG). In this study, it was observed that the absolute rate constant for their reaction with hydroxyl radicals increases in the order MeG < FCF < CV < MG. Total depollution of a dye mixture containing the above four dyes with a COD of 1000 mg L<sup>-1</sup> was also observed. Complete decolorization and approximately 85–90% mineralization of levafix red CA and levafix blue CA was observed by [El-Desoky et al. \(2010\)](#). Similar results were obtained in the cases of real dyeing wastewater ([Wang et al., 2010](#)), reactive blue 4 ([Gözmen et al., 2009](#)), direct orange 61 ([Hammami et al., 2007](#)), etc.

[Lin et al. \(2014\)](#) studied orange II removal behavior of EF process in a divided cell and reported that dye removal rate in cathodic compartment was much faster than that in anodic compartment. [Scialdone et al. \(2013\)](#) performed the abatement of acid orange 7 in a microfluidic reactor and reported that the process is efficient for the usage of cheaper and easier to handle graphite as cathodic material, mainly due to the sufficient oxygen production from the anode. Therefore, external addition of air or oxygen is not required for this type of reactor. [Iglesias et al. \(2013a\)](#) used airlift continuous reactor for the removal of reactive black 5 and lissamine green B and accomplished high decolorization percentages at high residence times. Methyl orange removal in a 3 L capacity pilot flow plant was studied by [Isarain-Chávez et al. \(2013\)](#) and obtained 80% of decolorization efficiency at the optimal conditions. Nanostructured ZnO-TiO<sub>2</sub> thin films deposited on graphite felt anode ([El-Kacemi et al., 2016](#)) exhibited higher dye removal and mineralization efficiency. Within 60 min of electrolysis Amido black 10B dye was discolored and the mineralization efficiency of the EF process reached 91% after 6 h of electrolysis. Application of graphene based electrode material improves the efficiency of EF process in a noticeable manner ([Yang et al., 2017](#)). Graphene ([Zhao et al., 2016](#)), graphene doped graphite-PTFE ([Xu et al., 2014](#)), reduced graphene oxide coated carbon felt ([Le et al., 2015](#)), graphite felt modified with

electrochemically exfoliated graphene (Yang et al., 2017) electrodes exhibited excellent hydrogen peroxide generation potential and subsequent dye removal efficiency.

Ferrous ion is the worldwide accepted Fenton catalyst for the generation of hydroxyl radical (Oturán and Aaron, 2014). Apart from this, other forms iron like zero-valent iron ( $\text{Fe}^0$ ) and ferric ions ( $\text{Fe}^{3+}$ ) can be used as Fenton catalyst. Addition of  $\text{Fe}^{3+}$  instead of  $\text{Fe}^{2+}$  undergoes the ferrous ion regeneration reaction prior to Fenton reaction.  $\text{Fe}^0$  addition leads to the production of  $\text{Fe}^{2+}$  by the reaction between hydrogen peroxide as in Eq. (22) (Fu et al. 2010a). Oturan et al. (2008a) used ferric ion instead of ferrous ion for the degradation of malachite green in Pt/CF cell at pH 3. The authors observed a total decolorization within 22 min and total mineralization within 540 min of electrolysis at an applied current of 200 mA. Özcan et al. (2009b) investigated the acid orange 7 removal by EF process using ferric ions and 92% of TOC removal was reported. Nidheesh and Gandhimathi (2014b) compared the RhB) removal efficiencies of  $\text{Fe}^0$ ,  $\text{Fe}^{2+}$  and  $\text{Fe}^{3+}$  in graphite-graphite EF system. The rate of dye removal at the optimal conditions follows the order of  $\text{Fe}^0 > \text{Fe}^{3+} > \text{Fe}^{2+}$ . But the optimum amount of Fenton's reagent followed the order of  $\text{Fe}^0 \sim \text{Fe}^{2+} > \text{Fe}^{3+}$ .



Persistent organic pollutant abatement using EF like process also received a great attention in recent years. The transition metals having more than one oxidation states and having a difference of unity in oxidation states can undergo Fenton like reactions as shown in Eq. (23). Various transition metals like Mn (Balci et al., 2009; George et al., 2014; Nidheesh and Gandhimathi, 2014b), Cu (Oturán et al., 2010b; George et al., 2013b; Nidheesh and Gandhimathi, 2014b), Co (Oturán et al., 2010b), Ag (Oturán et al., 2010b), Ni (George et al., 2014) etc. have been used as EF like catalyst for the abatement of various pollutants.



Recently, the EF related researches focused on the heterogeneous EF system (Nidheesh, 2015). In this process, solid catalysts containing iron species are used as the iron source instead of ferrous salts. Heterogeneous catalyst can be reused several times for the degradation of organic pollutants. Recently Oturan and co-workers proposed EF-pyrite process and found it to be very efficient for the mineralization of various organic pollutants (Amar et al., 2015; Barhoumi et al., 2015; 2016). Labiadh et al. (2015) used this technology for the removal of 4-amino-3-hydroxy-2-p-tolylazo-naphthalene-1-sulfonic acid, an azo dye from water medium and found complete mineralization of 175 mg L<sup>-1</sup> dye within 8 h of electrolysis. Nidheesh et al. (2014a) prepared magnetite by the chemical precipitation method and used for the decolorization of RhB. The authors used magnetite containing various concentrations of ferrous and ferric ions and found that the magnetite with Fe(II)/Fe(III) ratio 2:1 and 1:2 has good dye removal efficiency than other catalysts. At the optimal conditions, 97% of RhB was removed effectively by the heterogeneous EF process. Similarly EF oxidation of acid red 3R in the presence of Fe<sub>2</sub>O<sub>3</sub>/γ-Al<sub>2</sub>O<sub>3</sub> was investigated by Yue et al. (2014) and it was reported 77% dye removal within 100 min of electrolysis. Rosales et al. (2012) used Fe alginate gel beads for the removal of azure B and lissamine green B; and obtained almost complete removal of dyes from aqueous solution. Iglesias et al. (2013a) used the same catalyst for the decolorization of reactive black and lissamine green B 5 in an airlift continuous reactor. Iron loaded sepiolite was used as a heterogeneous EF catalyst for the removal of reactive black 5 in a continuous flow mode of operation (Iglesias et al., 2013b) and obtained 80 to 100% dye removal at the optimal conditions. Liang et al. (2016) investigated the effect of five metals (Cu, Ce, Mn, Fe and Co) and their loading contents on methyl orange degradation, observing the highest activity on Co/GDE and good stability toward wide pH ranges (3–9).

The dye removal mechanism of heterogeneous EF process is illustrated in Fig. 2. Iron species from the heterogeneous catalyst are released into the solution and reacts with the hydrogen peroxide produced at the cathode surface as in conventional Fenton process. In some of the cases, the Fenton reactions may occurs at the solid catalyst surface, without the dissolution of iron species. At these conditions the catalyst should be in suspension or efficient mixing should be there for the effective removal of organic pollutants.

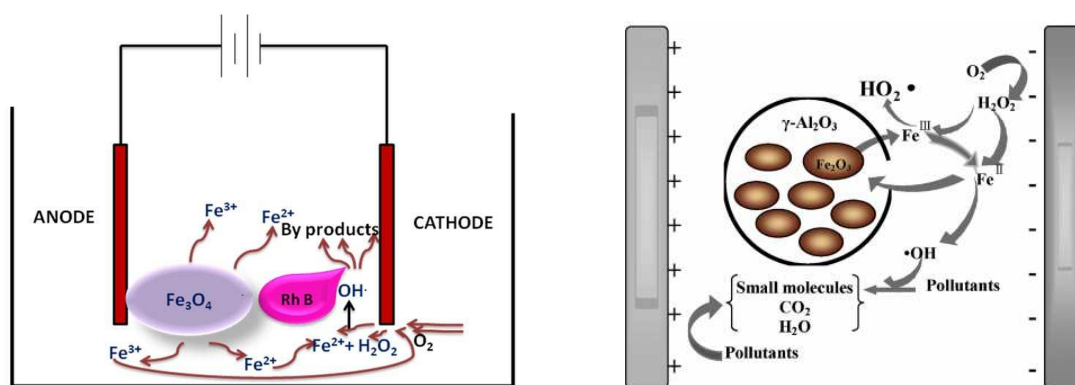


**Fig. 2** Dye removal mechanism of heterogeneous EF process using (a) magnetite (Nidheesh et al., 2014d), (b)  $\text{Fe}_2\text{O}_3/\gamma\text{-Al}_2\text{O}_3$  (Yue et al., 2014). Reprinted with permission from *RSC Adv.*, Copyright 2014 RSC and *J. Ind. Eng. Chem.*, Copyright The Korean Society of Industrial and Engineering Chemistry and Elsevier 2013, respectively.

Another trend in EF process is the application of three dimensional (3D) electrolytic cells for the abatement of persistent organic pollutants. 3D EF process is similar to the conventional two electrode system. But it contains particle electrode as the third electrode. Particle electrode is generally a granular material, which may contain iron oxides and filled between anode and cathode. Iron loaded inert substances and iron oxides can be used as the particle electrode for the EF system. Polarization of the particle electrode occurs during the electrolysis. Due to the polarization, these particles converts as a large numbers of charged microelectrodes with anode in one surface and cathode in other surface (Zhang et al., 2013).

These electrodes reduce the pollutant concentration by the sorption process, increasing the ionic strength of the electrolytic cell and supplying additional iron species in the system. In EF process, the particle electrodes predominately act as a heterogeneous EF catalyst (Wang et al., 2014a). Thus the efficiency of 3D EF system is higher than conventional EF system due to its large electrode surface and higher mass transfer (Wang et al., 2008a). The COD removal efficiency of 3D system should be 10-15% higher than that of conventional EF system (Zhang et al., 2013).

Zhang et al. (2014) used nanoscale zero-valent iron/activated carbon (NZVI/AC) as a heterogeneous Fenton catalyst in 3D EF system for the removal of methyl orange (MO). 20-30% of methyl orange mineralization efficiency increment was observed with the addition of the heterogeneous Fenton catalyst. More than 80% of dye removal efficiency after 10 min of electrolysis and 40% of TOC after 2 h of electrolysis were observed. Based on the experimental results, the authors proposed the degradation mechanism of MO in 3D EF system as in Fig. 3.

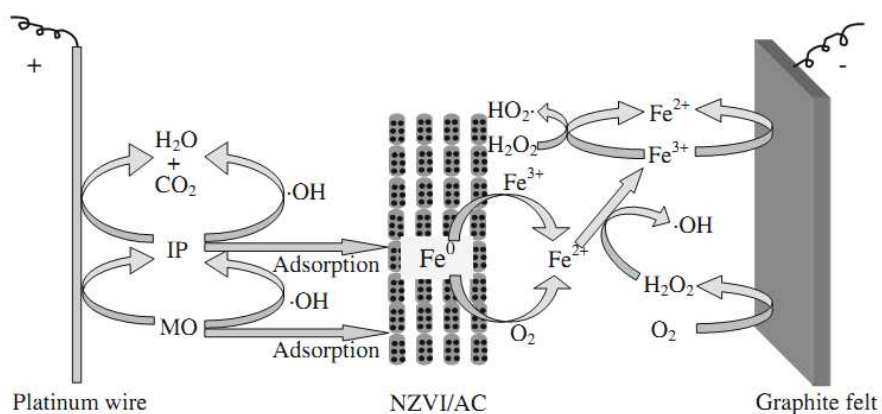


**Fig. 3** Methyl orange degradation mechanism in a 3D EF system (where, MO is methyl orange, NZVI/AC is nanoscale zero-valent iron/activated carbon and IP is intermediate products). Reprinted from Zhang et al. (2014), Copyright 2014, Springer-Verlag Berlin Heidelberg.

Wang et al. (2014b) used catalytic particle electrodes derived from steel slag and manganese loaded on the particle electrodes by ultrasound impregnation calcinations approach for the removal of RhB from aqueous solution by 3D EF process containing Pt anode and stainless steel cathode. The authors observed a complete removal of dye within 50 min of electrolysis. Electrolysis of real dyeing wastewater in the presence of graphite rings particle electrode, Pt/Ti plate anode and graphite cathode was carried out by Wang et al. (2008a). The authors attained a 70.6% color removal under specific operation conditions in 150 min. Wang et al. (2014a) used particle electrode prepared from steel slag for the removal of RhB and obtained 82.4% and 65.45% of RhB removal with and without of air supply within 60 min of electrolysis.

Removal of dyes from water medium using EF process under continuous flow mode was tested by Nidheesh and Gandhimathi (2015a, b). The authors used bubble column reactor (BCR) of capacity 3L for the removal of RhB from aqueous solution. They studied the effects of applied voltage, solution pH, catalyst concentration and inlet flow rate on the removal of dyes in continuous flow mode. At the optimal conditions, 98% of the RhB solution having an initial concentration of 50 mg L<sup>-1</sup> was removed effectively using the BCR under continuous flow mode. Similarly, EF process operated in BCR is highly efficient for the treatment of real textile wastewater (Nidheesh and Gandhimathi, 2015b). Due to the increased mass and electron transfer, flow-through EF reactor (in which solution is flow through anode and cathode) was found more energy-efficient and more pollutant removal efficiency than conventional EF reactor (Ma et al., 2016; Ren et al., 2016).

Even EF or related processes are very efficient for the abatement of various persistent organic pollutants from water medium; the incomplete mineralization of these pollutants may cause further environmental pollution. Some of the intermediate compounds are more toxic than their parent compounds. For example, Le et al. (2016) carried out the toxicity analysis

during the acid orange 7 degradation via EF process. In the initial periods of electrolysis, the toxicity values increased abruptly and are very much higher than that of acid orange 7. This is mainly due to the generation of more toxic intermediate products such as 1,2-naphthaquinone and 1,4-benzoquinone. The subsequent degradation of these compounds resulted in the production of carboxylic acids and decreased the toxicity values significantly. But, phytotoxicity and microbial toxicity of real textile wastewater has been reduced significantly after 1 h EF treatment (Roshini et al., 2017).

## 4.2 Peroxi-coagulation

Peroxi-coagulation is a modified EF process which use iron or stainless steel as anode for supplying ferrous ions in water medium, instead of external ferrous ion addition as in EF process. Ferrous ions continuously generated from anode by oxidation of a sacrificial anode according to Eq. (24). In the case of use an appropriate cathode able to generate H<sub>2</sub>O<sub>2</sub> and O<sub>2</sub> supply, Fenton's reaction takes place to form <sup>•</sup>OH. With the increase in electrolysis time, ferric ions accumulates in the aqueous medium leads to the formation of Fe(OH)<sub>3</sub> precipitate. Thus, peroxi-coagulation process is a combination of EF and electrocoagulation, in which organic pollutants are removed by the attack of hydroxyl radicals (degradation process) and coagulation with iron precipitates (Brillas and Casado, 2002). This process was firstly applied for the removal of aniline from aqueous medium (Brillas et al., 1997). The overall reactions occurring in a peroxi-coagulation cell along with organic pollutants removal mechanism are shown in Fig. 4.



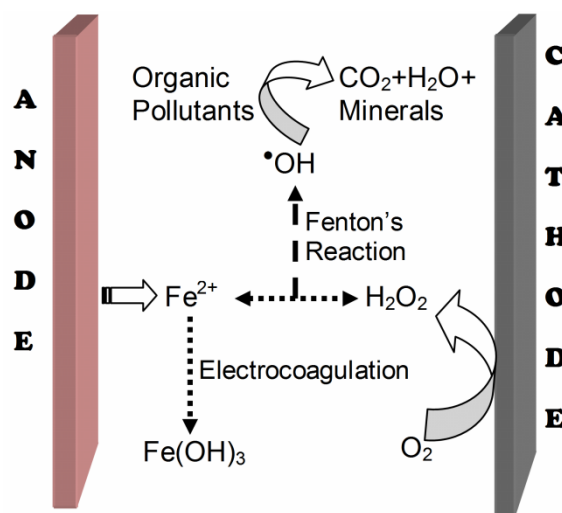


**Fig. 4** Working principles of peroxi-coagulation process

Increase in solution pH with electrolysis time is the difference in peroxi-coagulation with EF process (Venu et al., 2014, 2016). Hydrogen evolution reaction by the water reduction at the cathode surface (Eq. (25)) is the main reason behind the raise in solution pH (Drogui et al., 2008). This increase in pH increases also the rate  $\text{Fe(OH)}_3$  formation and causes electrocoagulative removal of pollutants along with oxidative action Fenton's reaction. This results in a higher amount of sludge production in the electrolytic cell. Brillas and Casado (2002) observed higher pollutant removal efficiency for peroxi-coagulation than EF process for currents  $\geq 10$  A and this is mainly attributed to the effective removal of intermediate compounds formed (by the attack of hydroxyl radicals) and by coagulation (adsorption or imprisonment in  $\text{Fe(OH)}_3$ ). The sludge formation in the peroxi-coagulation cell can be reduced by maintaining the solution pH to 3. At these conditions, the iron (III) concentration in the system is less than that of ferrous or ferric ions, results in Fenton's reaction to take place more efficiently.



A few studies have been reported for the dye removal by peroxi-coagulation process. Zarei et al. (2010a) used peroxi-coagulation process for the removal of four dyes namely C.I.

basic red 46, C.I. basic blue 3, C.I. basic yellow 2 and malachite green from aqueous solution at pH 3 and reported about 90% of dye removal within 10 min electrolysis. [Salari et al. \(2009\)](#) reported that peroxi-coagulation process has the ability to decolorize 90% of the dye in less than 30 min and 81% mineralization of dye at 6 h. Similar results were reported by [Zarei et al. \(2009\)](#).

Sludge formation in peroxi-coagulation process can be reduced by regulating the solution pH to 3. [Nidheesh and Gandhimathi \(2014 d\)](#) reported that pH regulated peroxi-coagulation has higher dye removal efficiency than that of pH unregulated peroxi-coagulation process. But the authors observed scavenging effects by the addition of sodium salts containing chloride, bicarbonate, carbonate and sulphate. For maintaining the pH, the authors used sulphuric acid and regulated the solution pH to 3 at every 15 min interval. This increased the concentration of sulphate ions in the cell. By the addition of sodium salts, higher amount of sulphate salts precipitate produces (as per common ion effect according to Le Chatelier's principle) and form a layer at the cathode surface. The authors observed a white layer formation on the cathode surface after the electrolysis, and this layer contains higher amount of sodium sulphates. This layer was removed with the insertion of cathode in an acid solution. Due to this layer formation, the volume of active pores at cathode surface reduces and results in lesser hydrogen peroxide formation. This causes a reduction in dye removal efficiency by the addition of sodium salts.

[Nidheesh and Gandhimathi \(2014c\)](#) compared the decolorization and degradation efficiencies of EF, peroxi-coagulation (PC) and pH-regulated peroxi-coagulation (PC-pH) processes from real textile wastewater. Based on the experimental results, the authors concluded that the color and COD removal efficiency of EF process is mainly by the oxidation of pollutants and the efficiency of peroxi-coagulation is mainly by the combination of oxidation and separation processes. The authors observed a higher sludge production for

PC and PC-pH processes at higher pH values and concluded that the higher removal efficiencies at higher pH values is mainly by electrocoagulation process. The sludge produced from PC process was reused as a heterogeneous EF catalyst for the abatement of same real textile wastewater and observed 97% of color, 47% of COD and 33.2% TOC reductions.

### 4.3 Fered-Fenton and Anodic Fenton processes

Fered-Fenton process is a modified form of Fenton process, in which hydrogen peroxide and ferrous ions are added externally to the electrolytic cell and then ferrous iron regenerated electrochemically from reduction of  $\text{Fe}^{3+}$  formed in Fenton's reaction (Eq. 15) for the improvement of process efficiency (Brillas et al., 2009). This process is also known as EF-Fere and is suitable for the abatement of organic pollutants with high TOC value and lower biodegradability. With the addition of hydrogen peroxide and ferrous iron salt, conventional Fenton's reaction occurs between ferrous ion and hydrogen peroxide and  $\cdot\text{OH}$  produced following Fenton's reaction (Eq. 15) results in the reduction of organic loading. Further reduction of organic pollutant can be attributed to conventional Fenton process assisted by electrochemistry since Fenton's reaction is catalyzed by the regeneration of ferrous ions from the electrochemical reduction of ferric ions (Brillas et al., 2009).

Anodic Fenton process is a Fenton related electrochemical peroxidation process. It can be considered as a modified form of peroxi-coagulation process. One of the major disadvantages of peroxi-coagulation process is the sludge production due to the formation of  $\text{Fe}(\text{OH})_3$  in excess of iron(III) in the solution. The main problem for this is the lack of sufficient quantity of hydrogen peroxide production at the cathode surface (As per conventional Fenton's reaction, the theoretical ratio of ferrous to hydrogen peroxide is 1. But

in peroxi-coagulation process, the concentration of ferrous ion increases and that of hydrogen peroxide comes to saturation or decreases with electrolysis time). This results in higher sludge formation and may cause scavenging reactions as given below (Brillas et al., 2009).



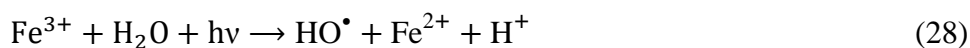
This can be reduced by the external addition of hydrogen peroxide, known as anodic Fenton process. Ghosh et al. (2012) studied the degradation of methylene blue and titan yellow dye solutions using this method (but authors mentioned it wrongly as EF process) and observed 98% and 96% respective dyes removal after 60 min of electrolysis at pH 3, 1 mM of  $\text{H}_2\text{O}_2$  and current density of  $4.31 \text{ mA cm}^{-2}$ . Eslami et al. (2013) compared the efficiencies of anodic Fenton process (but authors mentioned it wrongly as EF process) with conventional Fenton process for the removal of color and COD from real textile wastewater and higher removal efficiency for anodic Fenton process was observed. The decolorization and COD removal efficiencies of anodic Fenton process after 60 min of electrolysis were found as 72.9% and 70.6%, respectively, within 350 mA current and externally added  $1978 \text{ mg L}^{-1} \text{ H}_2\text{O}_2$  concentration. At the same time, 52.3% of color and 51.2% of COD were removed via Fenton process after 120 min of treatment at  $1978 \text{ mg L}^{-1} \text{ H}_2\text{O}_2$  concentration and  $250 \text{ mg L}^{-1}$  of ferrous ion concentration.

In order to improve the efficiency of anodic Fenton process and to reduce the negative effect of hydroxyl ions produced by the water reduction at cathode, Saltmiras and Lemley (2000) used divided electrolytic cell. Anode cell and cathode cell are connected with a salt bridge. Then the anode cell is enriched with the electrolytically generated ferrous ions and Fenton reactions occur with the external addition of hydrogen peroxide. Thus, anodic Fenton process reduces the external addition of large quantity of iron salts as in conventional Fenton

process and the effluent pH can be partially neutralized by combining the treated solutions from each cells (Wang and Lemley, 2002). But the scale up of anodic Fenton with a salt bridge is a little difficult task because the salt bridge requires frequent replacement of the saturated NaCl solution (Wang and Lemley, 2003). To overcome this, Lemley group developed membrane anodic Fenton process, in which an ion exchange membrane used between anode cell and cathode cell, instead of salt bridge.

#### 4.4 Photoelectro-Fenton process

A combination of UV radiation along with EF process, known as photoelectro-Fenton (PEF) process, produces more hydroxyl radicals than that in conventional EF process. This enhances the rate of dye degradation by the Fenton's reaction. The additional hydroxyl radicals are produced by the photochemical reduction of  $\text{Fe}^{3+}$  ions from UV light irradiation as in Eq. 28 (Brillas et al., 1998 a, b; Muruganandham and Swaminathan, 2004). On the other hand the regeneration of  $\text{Fe}^{2+}$  ions by this reaction (Eq. (28)) catalyzes also the Fenton's reaction (Eq. 15) to produce more  $\cdot\text{OH}$ . The photolysis of *in situ* produced  $\text{H}_2\text{O}_2$  in the presence of UV light also produces additional  $\cdot\text{OH}$  according to Eq. (29) (Brillas, 2014), but the amount of  $\cdot\text{OH}$  produced by this reaction is not significant because of very low absorption coefficient of  $\text{H}_2\text{O}_2$ .



Production of hydroxyl radicals and regeneration of ferrous ions from the photodegradation of iron complexes and ferric carboxylates is another advantage of PEF over conventional EF process. The photo-reduction of ferric hydroxyl complexes especially  $\text{Fe}(\text{OH})^{2+}$  produces additional  $\cdot\text{OH}$  as in Eq. 30 (Gogate and Pandit, 2004; Kavitha and Palanivelu, 2004; Brillas

2014). Similarly, photo-reactive ferric carboxylates also undergoes degradation process and produces additional ferrous ions and  $\cdot\text{OH}$  according to Eq. (31) (Brillas, 2014).

Many researchers put an interest on dye removal using PEF process. Khataee et al. (2014) compared the efficiency of EF and PEF processes for the abatement of C.I. Acid Blue 5 under recirculation mode with a cathode containing multi walled carbon nanotubes. The authors observed dye removals of 98% after 60 min of electrolysis for PEF processes. Similarly, Bedolla-Guzman et al. (2016) compared the efficiencies of anodic oxidation, EF and PEF processes for the degradation of Reactive Yellow 160 dye, using BDD anode. The authors observed dye removal efficiency order as: PEF>EF>anodic oxidation. Similar results are reported by Solano et al. (2015) for the degradation of Congo red dye and El-Ghenymy et al. (2015) for the abatement of malachite green oxalate dye. Khataee et al. (2010a) used carbon nanotube-polytetrafluoroethylene cathode for the removal of C.I. basic red 46 by the oxalate catalyzed PEF process and compared its efficiency with the efficiencies of EF and PEF processes. The authors reported that oxalate catalyzed PEF process has higher dye removal efficiency than that of PEF and EF process. Abatement of  $244 \text{ mg L}^{-1}$  Acid Red 29 by PEF process using BDD anode and carbon-PTFE cathode in an undivided cell was studied by Almeida et al. (2012) and observed an almost complete dye mineralization. Garcia-Segura et al. (2012) compared the Direct Yellow 4 degradation efficiencies of EF, PEF and photo-assisted EF process. Photo-assisted EF was performed by applying EF treatment for a particular time, followed by the photolysis of treated dye solution. They reported higher dye removal efficiency for PEF process (almost total mineralization). The authors also observed an equivalent dye removal capacity of PEF process for photo-assisted EF process after giving sufficient time for the EF process to produce intermediates that can be mineralized by the photolysis. Peralta-Hernández et al. (2008) compared the Orange II removal efficiencies of direct photolysis, EF and PEF processes and observed 31%, 63% and 83% of TOC removals,

respectively. Mineralization of Acid Red 14 by PEF process using an activated carbon fiber cathode was examined by Wang et al. (2008b) and compared its efficiency with EF process. The authors observed 60–70% mineralization efficiency for EF process and more than 94% mineralization efficiency for PEF process. Mineralization and decolorization of aqueous solution containing Acid Violet 7 and Reactive Black 5 by EF and PEF processes using a vitreous carbon electrode cathode was studied by Salazar and Ureta-Zañartu (2012) and observed more than 90% mineralization efficiency for PEF process.

The pseudo first order rate of dye removal by PEF process was modeled as a function of catalyst concentration, initial dye concentration, solution pH, applied current and flow rate by Khataee et al. (2014). The authors reported the rate constant as:

$$k_{app} = 1310.4 \frac{[CA]^{0.48} I^{0.55}}{[Dye]^{1.07} pH^{1.75} Q^{0.84}} \quad (32)$$

where,  $k_{app}$  is the apparent rate constant following first order kinetic, CA is the catalyst concentration in mM,  $I$  is the applied current in A,  $Q$  is the flow rate in L h<sup>-1</sup>.

Coupling of conventional photocatalysis with PEF process received great attention in recent years. The principles of photocatalysis were explained well by various researchers (Bahнемann, 2004; Girish Kumar and Gomathi Devi, 2011; Rauf et al., 2011; Lam et al., 2012). Iranifam et al. (2011) used ZnO nanoparticles as the photo catalyst for the removal of C.I. Basic Yellow 28 from aqueous solution and compared the dye removal efficiencies of ultraviolet-C (UV-C), EF, UV/ZnO, PEF and PEF/ZnO processes. The authors found the decreasing color removal efficiency order as: PEF/ZnO > PEF > UV/ZnO > EF > UV-C. Similarly, Khataee and Zarei (2011) reported the C.I. Direct Yellow 12 removal efficiency order as: PEF/ZnO > PEF > EF > UV/ZnO. Photocatalytic treatment of C.I. Acid Red 17 using immobilized TiO<sub>2</sub> nanoparticles combined with PEF process was investigated by Khataee et al. (2010b) and it was observed the color removal decreasing order as: PEF/UV/TiO<sub>2</sub> > PEF >

EF > UV/TiO<sub>2</sub>. The authors observed 93.7%, 85.9%, 66.8% and 20% decolorization efficiencies for PEF/UV/TiO<sub>2</sub>, PEF, EF and UV/TiO<sub>2</sub> processes respectively. Similar order was reported by Zarei et al. (2010b) for the removal of C.I. Basic Red 46. The authors observed 98.8% mineralization of 20 mg L<sup>-1</sup> C.I. Basic Red 46 dye at 6 h of electrolysis using PEF/TiO<sub>2</sub> process.

#### 4.5 Solar Photoelectro-Fenton

PEF process has been found as an effective tool for the abatement of dyes from water medium. But the higher energy consumption of artificial UV light used in PEF process increases the operational cost of this process (Brillas, 2014). In order to solve this disadvantage of PEF process and to increase the chance of applying this process in the real field, Brillas' group (Flox et al., 2007a, 2007b) proposed a modified form of PEF process, known as solar photoelectro-Fenton (SPEF) process for the degradation and removal of various organic persistent pollutants. In this process, the EF treated wastewater is irradiated with sunlight ( $\lambda > 300$  nm), instead of artificial UV light as in PEF process. Therefore, SPEF method is cheap, uses renewable energy source, high energy efficient, amenable to automation, versatile and safe (Martínez-Huitle and Brillas, 2009; Brillas, 2014). It is also found that the efficiency of SPEF is higher than that of PEF process due to the greater intensity of UVA and UVB lights of sunlight which can photolyze the ferric carboxylate complexes more rapidly (Garcia-Segura et al., 2013; Brillas, 2014). Also, compared to EF process, SPEF process is more potent than EF, with higher mineralization efficiency, higher current efficiency and lower energy consumption (Salazar et al., 2011). Garcia-Segura and Brillas (2016) compared the performance of SPEF for the degradation of monoazo, diazo and triazo dyes in water medium. Acid Orange 7, Acid Red 151 and Disperse Blue 71 were considered as the model monoazo, diazo and triazo dyes, respectively. SPEF process is very

much efficient for the degradation of monoazo dye with almost complete mineralization after 3 h of electrolysis. At the same time, the dye degradation efficiency of SPEF is high for triazo dye than diazo dye.

[Ruiz et al. \(2011a\)](#) used 2.5 L flow plant for the degradation of Acid Red and Acid Yellow from water medium. The electrolytic cell was equipped with carbon-PTFE cathode and BDD anode. The solar photo-reactor having irradiated volume of 600 mL and containing mirror at bottom with a horizontal inclination of  $30^0$ . The authors observed a rapid decolorization of both dyes by the EF process, but the mineralization rate was low. This low mineralization rate of EF process is mainly due to the higher concentration of persistent carboxylic acids and their iron-complexes. But the photolysis of this electrolyzed solution leads to almost total mineralization of dye wastewater. [Ruiz et al. \(2011b\)](#) used same reactor for the removal of Acid Yellow 36 from aqueous solution and observed the similar results as explained above. Degradation of Disperse Red 1 and Disperse Yellow 3 using SPEF process was examined by [Salazar et al. \(2011\)](#) and observed total mineralization of both dyes.

#### **4.6 Sonoelectro-Fenton:**

Application of ultrasound for the treatment of water and wastewater received a great attention during the recent years ([Gogate et al., 2002](#); [Sivasankar and Moholkar, 2010](#); [Bagal and Gogate, 2014](#)). Acoustic cavitation is the forcing phenomenal for the degradation of organic pollutants in the presence of ultrasound in water medium. It is the process of formation, growth, and succeeding collapse of microbubbles or cavities due to ultrasound in a water medium ([Gogate and Pandit, 2004](#)). The collapse of bubbles occurs within 50 ns, and the process is almost adiabatic ([Chakma and Moholkar, 2013](#)), results in the generation of higher pressure (in the range of 500–5,000 bar) and temperature (in the range of 1,000–

15,000 K) in the reactor (Suslick, 1989). Due to this cavitation phenomenon, hydroxyl radicals are formed as given below (Li et al., 2010).



where U.S. refers to the application of ultrasound.

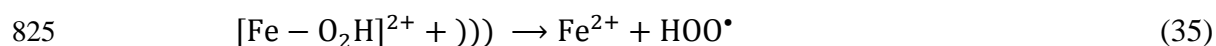
Addition of ultrasound in EF process, known as sonoelectro-Fenton (SEF) process (Oturán et al., 2008b), results in a higher amount of radicals in the water medium and thus higher removal efficiency than EF process. In the presence of ultrasound, the electrolytically produced hydrogen peroxide dissociated into hydroxyl radicals as:



Oturán et al. (2008b) reported the order of relevance of the enhancing factors in SEF process as: (1) enhanced production of hydroxyl radical and Fenton reaction kinetics by the improved mass transfer rate of both reactants (ferric ions and oxygen) towards the cathode surface for the electrochemical generation of Fenton's reagent and its transfer into the solution, (2) the additional hydroxyl radical generation by the sonolysis, and (3) pyrolysis of organics at the time of bubble explosion.

Li et al. (2010) observed an increased hydrogen peroxide production with the addition of ultrasound in EF cell. The hydrogen peroxide produced in SEF process is higher than the sum of hydrogen peroxide concentration produced from EF and sono Fenton processes. This improvement can be related to enhancement of mass transfer by sonolysis Oturán et al. (2008b).

In the presence of ultrasound, the regeneration of ferrous ions from intermediate complex produced via conventional Fenton process also occurs as in Eq. (35) (Pradhan and Gogate, 2010; Bagal and Gogate, 2014). This results in an enhancement of Fenton reactions in the electrolytic cell.



The arrangement of sono probe (one type of ultrasound source) and electrode also affects the efficiency of SEF process. There are three types of probe-electrode arrangement ([Compton et al., 1997](#)) in a sono-electrochemical reactor, namely face-on, side-on and sonotrode. Among this arrangement, face-on orientation has higher mass transfer capability and is depends on ultrasound power, electrode-horn distance and electrode area ([Ramachandran and Saraswathi, 2011](#)). These authors also tested the efficiency of angular geometry and compared with that of face-on orientation. But the mass flux values of face-on orientation are two to three times higher than that of angular geometry. Thus, face-on geometry is the better probe-electrode arrangement in a SEF reactor. This arrangement reduces the layer formation on the cathode surface and enhances the efficiency of SEF process. Thus the enhancement in the efficiency of SEF process is mainly due to physical and chemical mechanisms ([Babuponnusami and Muthukumar, 2012](#)). Physical mechanism related to the high mixing and electrode surface cleaning by the addition of ultrasound in the EF reactor. This enhances the mass transfer between electrode and solution in addition to higher hydrogen peroxide production. The chemical mechanism is due to the additional radical formation in the cell as explained above.

SEF process has been found as an efficient tool for the abatement of dyes from aqueous solution. An enhancement in hydrogen peroxide production and dye removal rate with the addition of ultrasound in EF process was observed by [Li et al. \(2010b\)](#). Authors concluded that in SEF process, low frequency ultrasound has a positive effect on dye mineralization. The rate of dye removal by SEF process is 10 fold higher than that of sonolysis and 2 fold higher than that of conventional Fenton process ([Martínez and Uribe, 2012](#)). Abatement of reactive blue 19 dye using SEF process was investigated by [Siddique et al. \(2011\)](#). The authors observed an almost complete removal of dye and 56.47% of TOC from unhydrolyzed reactive blue 19 dye solution at a frequency of 80 kHz. At the same time, 81% of

TOC removal was observed for hydrolyzed reactive blue 19 solution. Similar way, 85% of TOC and more than 90% of color introduced by azure B were removed efficiently by SEF process in the presence of reticulated vitreous carbon cathode and platinum gauze counter electrode (Martínez and Uribe, 2012). Oturan et al. (2008b) observed a synergistic effect in SEF process (compared to EF process) in degradation of azobenzene at low frequencies (i.e. 20 and 60 80 kHz) and an improvement in degradation kinetics for early treatment times. Similarly, Şahinkaya (2013) observed a negligible increase in treatment efficiency of SEF process, when compared with the capital and operating costs of sonication. Lounis et al. (2016) examined the performance of SEF for the degradation of Orange G in various water mediums like pure water, natural water and seawater. The dye removal rate was very high in sea water medium followed by pure water and natural mineral water. Complete dye removal was observed for sea water and pure water medium, while 94% of dye removal was observed for natural mineral water medium.

#### 4.7 Bioelectro Fenton

Two versions of bioelectro-Fenton were reported: (i) bioelectro-Fenton (BEF) based on bio-electrochemical reactor proposed by Zhu and Ni (2009) consisting of two cells: microbial fuel cell (MFC) containing biodegradable organic substrates and anodic Fenton treatment (AFT) cell containing pollutants to be degraded by EF process, and (ii) BEF consisting of coupling between EF process and microbial degradation (Olvera-Vargas et al., 2016a, b). EF step being utilized as pre-treatment for mineralization of beta-blocker drug metoprolol: 1 h EF pre-treatment step followed by aerobic biodegradation allowed 90% mineralization at 4 days. On the other hand, Ganzenko et al., (2017) investigated the use of BEF during treatment of a pharmaceutical wastewater treatment in two scenarios: EF as both pre-

treatment and post-treatment of biological step and found and found first scenario more efficient.

[Feng et al. \(2010b\)](#) used BEF system containing anaerobic anode chamber having *Shewanella decolorationis* S12 as microorganism for the generation of electricity and carbon nanotube (CNT)/ $\gamma$ -FeOOH composite cathode for the production of hydrogen peroxide. The authors used this system for the abatement of orange II and observed a complete decolorization and mineralization of dye. A maximum power output of  $230 \text{ mW m}^{-2}$  was also obtained from the BEF system. But modification of BEF system with polypyrrole/anthraquinone-2,6-disulfonate (PPy/AQDS) conductive film boosted the performance of the system. [Feng et al. \(2010a\)](#) observed a maximum power density of  $823 \text{ mW m}^{-2}$  by the use this conductive film.

MFC is a “renewable energy device that converts energy available in organic compounds to electricity via the canalization of microorganisms” ([Feng et al., 2010a](#)). The biodegradable organic substance generally used in an MFC is glucose or acetate. Microorganisms present on the anode compartment oxidize these substrates and generates protons and electrons ([Zhu and Logan, 2013](#)). The electrons produced via this oxidation process flow through an external circuit to cathode. At the same time, the protons released into the solution. At the cathode surface, oxygen reacts with both proton and electron, forms water as in [Eq. \(36\)](#).



Besides the electricity generation, MFC have several other advantages. Self-regeneration capacity of microorganism reduces the catalyst cost in MFC compared to conventional chemical fuel cells ([Fernándezde Dios et al., 2013](#)). Absence of pollutant generation

(including all toxic substances) during any operations in MFC makes this cell as an environmentally friendly energy system (Gong et al., 2011).

Rabaey and Rozendal, (2010) showed that a MFC can generate a voltage of 0.8 V to an open circuit and this low-voltage electricity can be used for other electrolytic process like hydrogen peroxide production in EF process. By this reaction, 78.85 mg L<sup>-1</sup> of H<sub>2</sub>O<sub>2</sub> production in the cell after 12 h of electrolysis was observed by Fu et al. (2010b). This hydrogen peroxide undergoes conventional Fenton's reaction and produces <sup>•</sup>OH. But in BEF, the production of hydrogen peroxide requires only two-electron transfer. Thus a BEF system generates electricity, produces <sup>•</sup>OH in cathodic compartment and causes degradation of organic pollutants. The working principles of a BEF system are shown in Fig. 5.

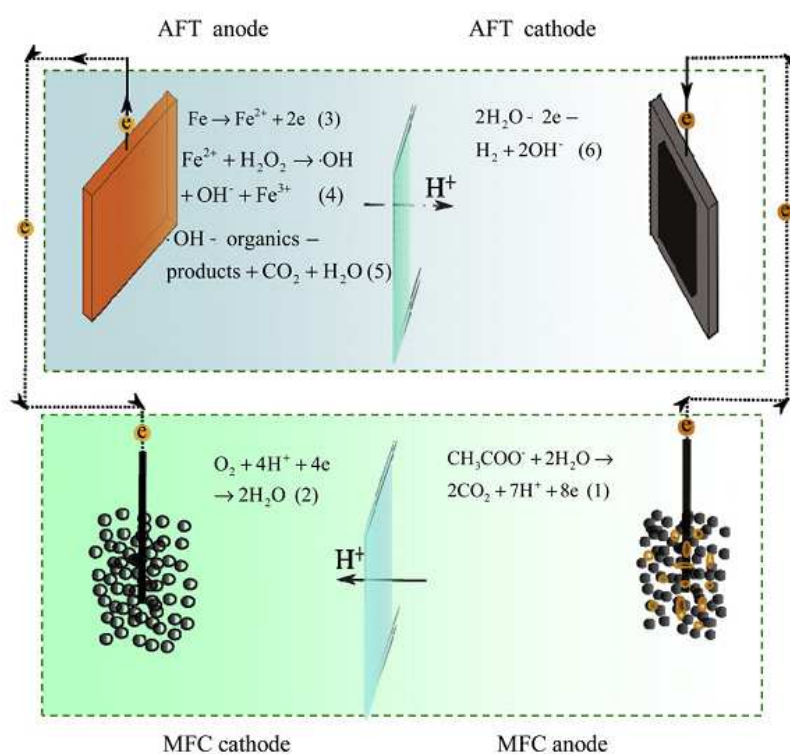


**Fig. 5** Energy generation and subsequent pollutant removal reactions in MFC assisted-AFT system. Reprinted with permission from Liu et al., (2012). Copyright 2012, Elsevier.

Effect of MFC combined with *in situ* and *ex situ* EF processes on the abatement of dye was examined by [Fernández de Dios et al. \(2013\)](#). The authors carried out the experiments both in batch and continuous flow mode for the removal of lissamine green B and crystal violet from aqueous solution. 94% of lissamine green B and 83% of crystal violet removals were observed by the researchers after 9 h of electrolysis in MFC combined with *in situ* EF process. For this condition, respective TOC amounts of 82% and 70% were removed from the same BEF reactor respectively for lissamine green and crystal violet. At the same time more than 95% of dye removal and 85% of TOC removal were observed in a bubble column reactor used in MFC combined with *ex situ* EF process.

Recently, [Zhang et al. \(2015\)](#) developed a new BEF reactor capable of supplying hydrogen peroxide and eliminating its residual concentration ([Fig. 6](#)). The investigators achieved this by alternating switching between microbial electrolysis cell (MEC) and microbial fuel cell (MFC). In MEC mode of operation, degradation of pollutants occurs by the electrolytic generation of  $H_2O_2$  and subsequent generation of hydroxyl radicals by the reaction with ferrous ions. The residual hydrogen peroxide after the MEC mode of operation consumes during the MFC mode of operation, by using hydrogen peroxide as electron acceptor. The authors tested the efficiency of this BEF system for the abatement of  $50\text{ mg L}^{-1}$  methylene blue solution. Almost complete decolorization and mineralization of the dye solution were achieved after 8 h and 16 h in MEC mode of operation. The residual hydrogen peroxide concentration was observed as  $180\text{ mg L}^{-1}$  and this was consumed completely in MFC mode of operation within 39 h of operation.

Coupling EF and microbial oxidation process is effective for treating real textile wastewater ([Roshini et al., 2017](#)). Combined EF and aerobic-microaerophilic process is able to remove 86.4% COD, 85.8% color and 56.1% TOC of textile wastewater. Similarly, 82.5%

COD, 52.7% color and 41% TOC were removed by EF process followed by aerobic microbial process..

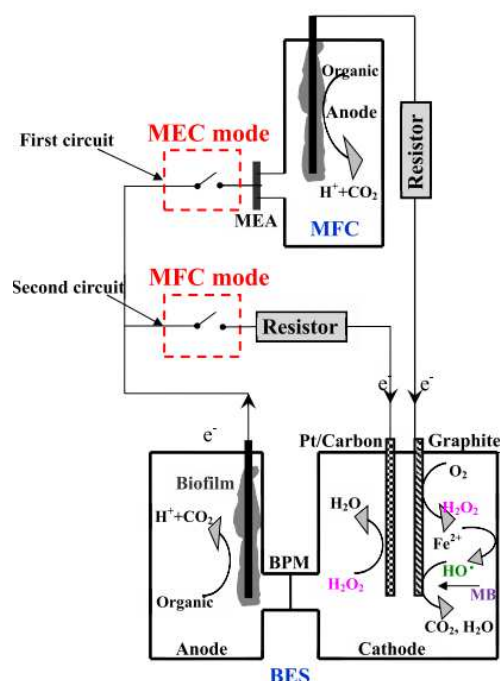


**Fig. 6** BEF reactor with alternate switching, where MEC: microbial electrolysis cell; MFC: microbial fuel cell; MEA: membrane electrode assembly; BES: bioelectrochemical system; BPM: bipolar membrane. Reprinted with permission from Zhang et al. (2015). Copyright 2015, Elsevier

## 5. Scale up of EAOPs cells

Application of EAOPs for the abatement of dyes was largely investigated at lab scale. A few studies were investigated even in continuous flow mode of operation, which resembles the practical conditions for the dye wastewater treatment. The next step of investigation is pilot scale studies for dye removal by EAOPs. The scale up of an electrolytic reactor depends on its geometric, kinematic, current/potential and thermal similarity between the reactors (Gupta and Oloman, 2006). Geometric similarity can be achieved by keeping the dimensional ratios as constant. But it is not advisable to increase the inner electrode spacing. Because, with increase in electrode spacing, the ohmic drop between electrodes increases, which

results in reduction in the efficiency of EAOPs. The increased spacing requires higher voltages for the optimal operation and this increases the energy consumption of the cell, consequently increases the cost of operation. Therefore, during scale up process of electrolytic reactors, geometric similarity is usually sacrificed in favor of current/potential similarity (Gupta and Oloman, 2006). Current/potential similarity is also known as electrical similarity; which can be achievable by keeping constant differences in electrode potential and current density (Goodridge and Scott, 1994). This can be achieved by keeping a constant inner electrode gap during scale up process. The kinematic similarity depends on the inlet flow rate and this similarity can be achievable by keeping same residence time or flow rate during the scale up process. Thermal similarity is another important parameter to be considered during the scale up process. Most of the lab scale works were carried out at the room temperature. But the effluents from the textile industry have the temperature near to the 100 °C. Therefore, a mismatching between the lab scale efficiency and real field efficiency will occurs. Because in the case of Fenton based EAOPs, the elevated temperature decreases the stability of oxygen and hydrogen peroxide. This decreases the efficiency of EAOPs at elevated temperature.

## **6. Conclusions and perspectives**

EAOPs have a great potential to remove dyes from water medium. Comparing to direct EAOPs, indirect EAOPs, especially that based on Fenton chemistry has received increased attention in the last decade. AO process, a well-known direct EAOPs, is also very efficient to remove dyes from aqueous solution. The higher cost of high oxygen over potential anode is one of the main drawbacks of this process. Various types of Fenton process based EAOPs, naming EF, PEF, SEF, peroxi-coagulation, fered Fenton, anodic Fenton etc. have been applied effectively for the removal of dyes. Total decolorization of dyes has been achieved in

most of the cases. But the mineralization efficiency is, in general, less than that of decolorization efficiency. This is mainly due to the less degradation rate of by-products in all the EAOPs. Ferrous ion is found as an efficient catalyst among various forms of iron for the removal of dyes in EF and related processes. EF like reactions, heterogeneous EF and 3D EF processes are the new trends in dye removal by EF based processes. The external addition of iron salt has been replaced with sacrificial iron anode in peroxi-coagulation process. But the sludge production and increased passivation rate of electrodes decreases the degradation efficiency of this process. The efficiency of EF process has been increased significantly by the addition of UV light (PEF) and ultrasound (SEF). The rate of removal of PEF and SEF processes are generally higher than that of EF process, but these latest processes are more costly because of coupling with highly energy consuming processes. The practical implementation of PEF process has been simplified by the introduction of solar energy (SPEF). Combined biological process and EAOPs is also a new trend in this field. In BEF, electricity produced from MFC has been used for the production of hydroxyl radicals. But the time taken for the removal of dyes by BEF is much higher than that of EF process.

Scale up of EAOPs is a global problem, even though these processes are very efficient and cheap. Electrical similarity is the major factor to be remembered during scale up operations. Since, this is very important for the real implementation of EAOPs, more works on dye removal by EAOPs in industrial scale is required. Overall, it can be concluded that EAOPs constitute a promising technology for the removal of dyes from aqueous solution.

## References

- Abdessamad, N., Akrouit, H., Hamdaoui, G., Elghniji, K., Ksibi, M., Bousselmi, L., 2013. Evaluation of the efficiency of monopolar and bipolar BDD electrodes for electrochemical oxidation of anthraquinone textile synthetic effluent for reuse. *Chemosphere* 93, 1309–1316.
- Abo-Farha, S.A., 2010. Comparative study of oxidation of some azo dyes by different advanced oxidation processes: Fenton, Fenton-like, photo-Fenton, and photo-Fenton-like. *J. Am. Sci.* 6 (10), 128–142.
- Almeida, L.C., Garcia-Segura, S., Arias, C., Bocchi, N., Brillas, E., 2012. Electrochemical mineralization of the azo dye acid red 29 (Chromotrope 2R) by photoelectro-Fenton process. *Chemosphere* 89 (6), 751–758.
- Almomani, F., Baranova, E.A., 2013. Kinetic study of electro-Fenton oxidation of azo dyes on boron-doped diamond electrode. *Environ. Technol.* 34 (11), 1473–1479.
- Ammar, S., Oturan, M.A., Labiadh, L., Guersalli, A., Abdelhedi, R., Oturan, N., Brillas, E., 2015. Degradation of tyrosol by a novel electro-Fenton process using pyrite as heterogeneous source of iron catalyst. *Water Res.* 74, 77–87.
- An, H., Cui, H., Zhang, W., Zhai, J., Qian, Y., Xie, X., Li, Q., 2012. Fabrication and electrochemical treatment application of a microstructured  $\text{TiO}_2\text{-NTs/Sb-SnO}_2\text{/PbO}_2$  anode in the degradation of C.I. reactive blue 194 (RB 194). *Chem. Eng. J.* 209, 86–93.
- Andrade, L.S., Tasso, T.T., da Silva, D.L., Rocha-Filho, R.C., Bocchi, N., Biaggio, S.R., 2009. On the performances of lead dioxide and boron-doped diamond electrodes in the anodic oxidation of simulated wastewater containing the reactive orange 16 dye. *Electrochim. Acta* 54 (7), 2024–2030.
- Anglada, A., Urtiaga, A., Ortiz, I., 2009. Contributions of electrochemical oxidation to wastewater treatment: fundamentals and review of applications. *J. Chem. Technol. Biotechnol.* 84 (12), 1747–1755.
- Aquino, J.M., Rocha-Filho, R.C., Rodrigo, M.A., Sáez, C., Cañizares, P., 2013. Electrochemical degradation of the reactive red 141 dye using a boron-doped diamond anode. *Water Air Soil Pollut.* 224, 1397.
- Aquino, J.M., Rodrigo, M.A., Rocha-Filho, R.C., Saez, C., Cañizares, P., 2012. Influence of the supporting electrolyte on the electrolyses of dyes with conductive-diamond anodes. *Chem. Eng. J.* 184, 221–227.
- Arivoli, S., Thenkuzhali, M., Martin Deva Prasath, P., 2009. Adsorption of rhodamine B by acid activated carbon- Kinetic, thermodynamic and equilibrium studies. *Orbital* 1 (2), 138–155.
- Babuponnusami, A., Muthukumar, K., 2012. Advanced oxidation of phenol: A comparison between Fenton, electro-Fenton, sono-electro-Fenton and photo-electro-Fenton processes. *Chem. Eng. J.* 183, 1–9.

- 1034 Bae, J.-S., Freeman, H.S., 2007. Aquatic toxicity evaluation of copper-complexed direct dyes  
1035 to the *Daphnia magna*. *Dyes Pigments* 73 (1), 126-132.
- 1036 Bagal, M.V., Gogate, P.R., 2014. Wastewater treatment using hybrid treatment schemes  
1037 based on cavitation and Fenton chemistry: A review. *Ultrason.Sonochem.* 21 (1), 1–14.
- 1038 Bahnemann, D., 2004. Photocatalytic water treatment: solar energy applications. *Sol. Energy*  
1039 77 (5), 445–459.
- 1040 Balci, B., Oturan, M.A., Oturan, N., Sirés, I., 2009. Decontamination of aqueous glyphosate,  
1041 (aminomethyl) phosphonic acid, and glufosinate solutions by electro-Fenton-like process  
1042 with  $Mn^{2+}$  as the catalyst. *J. Agr. Food Chem.*, 57(11), 4888-4894.
- 1043 Barhoumi, N., Labiadh, L., Oturan, M.A., Oturan, N., Gadri, A., Ammar, S., Brillas, E.,  
1044 2015. Electrochemical mineralization of the antibiotic levofloxacin by electro-Fenton-  
1045 pyrite process. *Chemosphere* 141, 250–257.
- 1046 Barhoumi, N., Oturan, N., Olvera-Vargas, H., Brillas, E., Gadri, A., Ammar, S., Oturan,  
1047 M.A., 2016. Pyrite as a sustainable catalyst in electro-Fenton process for improving  
1048 oxidation of sulfamethazine. *Kinetics, mechanism and toxicity assessment. Water Res.* 94,  
1049 52–61.
- 1050 Barredo-Damas, S., Alcaina-Miranda, M.I., Iborra-Clar, M.I., Bes-Pia, A., Mendoza-Roca,  
1051 J.A., Iborra-Clar, A., 2006. Study of the UF process as pretreatment of NF membranes for  
1052 textile wastewater reuse. *Desalination* 200 (1-3), 745–747.
- 1053 Bedolla-Guzman, A., Sirés, I., Thiam, A., Peralta-Hernández, J.M., Gutiérrez-Granados, S.,  
1054 Brillas, E., 2016. Application of anodic oxidation, electro-Fenton and UVA photoelectro-  
1055 Fenton to decolorize and mineralize acidic solutions of Reactive Yellow 160 azo dye.  
1056 *Electrochim. Acta* 206, 307–316
- 1057 Benfield, L.D., Weand, B.L., Judkins, J.F., 1982. *Process chemistry for water and wastewater*.  
1058 Prentice Hall Inc, Englewood Cliffs, New Jersey.
- 1059 Bensalah, N., Quiroz Alfaro, M.A., Martínez-Huitle, C.A., 2009. Electrochemical treatment  
1060 of synthetic wastewaters containing Alphazurine A dye. *Chem. Eng. J.* 149, 348–352.
- 1061 Bogdanowicz, R., Fabiańska, A., Golunski, L., Sobaszek, M., Gnyba, M., Ryl, J., Darowicki,  
1062 K., Ossowski, T., Janssens, S.D., Haenen, K., Siedlecka, E.M., 2013, Influence of the  
1063 boron doping level on the electrochemical oxidation of the azo dyes at Si/BDD thin film  
1064 electrodes. *Diam. Relat. Mater.* 39, 82–88.
- 1065 Braga, N.A., Cairo, C.A.A., Matsushima, J.T., Baldan, M.R., Ferreira, N.G., 2010.  
1066 Diamond/porous titanium three-dimensional hybrid electrodes. *J. Solid State Electrochem.*  
1067 14, 313-321.
- 1068 Brillas, E., 2014. A Review on the degradation of organic pollutants in waters by UV  
1069 photoelectro-Fenton and solar photoelectro-Fenton. *J. Braz. Chem. Soc.* 25 (3), 393-417.
- 1070 Brillas, E., Casado, J., 2002. Aniline degradation by electro-Fenton and peroxi-coagulation  
1071 processes using a flow reactor for wastewater treatment. *Chemosphere* 47 (3), 241–248.

- 1072 Brillas, E., Mur, E., Casado, J., 1996. Iron(II) catalysis of the mineralization of aniline using  
1073 a carbon-PTFE O<sub>2</sub>-fed cathode. *J. Electrochem. Soc.* 143 (3), L49–L53.
- 1074 Brillas, E., Mur, E., Sauleda, R., Sanchez, L., Peral, J., Domenech, X., Casado, J., 1998.  
1075 Aniline mineralization by AOP's: anodic oxidation, photocatalysis, electro-Fenton and  
1076 photoelectro-Fenton processes. *Appl. Catal. B-Environ.* 16, 31-42.
- 1077 Brillas, E., Sauleda, R., Casado, J., 1997. Peroxi-coagulation of aniline in acidic medium  
1078 using an oxygen diffusion cathode. *J. Electrochem. Soc.* 144 (7), 2374 – 2379.
- 1079 Brillas, E., Sauleda, R., Casado, J., 1998. Degradation of 4-chlorophenol by anodic oxidation,  
1080 electro-Fenton, photoelectro-Fenton, and peroxi-coagulation processes. *J. Electrochem.*  
1081 *Soc.*, 145, 759-765.
- 1082 Canizares, P., Gadri, A., Lobato, J., Nasr, B., Paz, R., Rodrigo, M.A., Saez, C., 2009.  
1083 Electrochemical oxidation of azoic dyes with conductive-diamond anodes. *Ind. Eng.*  
1084 *Chem. Res.* 45 (10), 3468-3473.
- 1085 Chakma, S., Moholkar, V.S., 2013. Physical mechanism of sono-Fenton process. *AIChE J.* 59  
1086 (11), 4303–4313.
- 1087 Chen, G., 2004. Electrochemical technologies in wastewater treatment. *Sep. Purif. Technol.*  
1088 38 (1), 11–41.
- 1089 Chen, X., Chen, G., Yue, P.L., 2003. Anodic oxidation of dyes at novel Ti/B-diamond  
1090 electrodes. *Chem. Eng. Sci.* 58 (3-6), 995 – 1001.
- 1091 COINDS, 2000. Comprehensive industry documents series on textile industry. Central  
1092 Pollution Control Board, India 59, 1999–2000.
- 1093 Comninellis, C., 1994. Electrocatalysis in the electrochemical conversion/combustion of  
1094 organic pollutants for waste water treatment. *Electrochim. Acta* 39 (11–12), 1857–1862.
- 1095 Comninellis, C., De Battisti, A., 1996. Electrocatalysis in anodic oxidation of organics with  
1096 simultaneous oxygen evolution. *J. Chim. Phys.* 93 (4), 673-679.
- 1097 Compton, R.G., Eklund, J. C., Marken, F., 1997. Sonoelectrochemical Processes: A review.  
1098 *Electroanal.* 9 (7), 509-522.
- 1099 Couto, S.R., 2009. Dye removal by immobilised fungi. *Biotechnol. Adv.* 27 (3), 227–235.
- 1100 Crini, G., 2006. Non-conventional low-cost adsorbents for dye removal: A review.  
1101 *Bioresource Technol.* 97 (9), 1061–1085.
- 1102 Demirbas, A., 2009. Agricultural based activated carbon for the removal of dyes from  
1103 aqueous solutions: A review. *J. Hazard. Mater.* 167 (1-3), 1–9.
- 1104 Diagne, M., Sharma, V.K., Oturan, N., Oturan, M.A., 2014. Depollution of indigo dye by  
1105 anodic oxidation and electro-Fenton using B-doped diamond anode. *Environ. Chem. Lett.*  
1106 12, 219–224.
- 1107 do Vale-Júnior, E., Dosta, S., Cano, I.G., Guilemany, J.M., Garcia-Segura, S., Martínez-  
1108 Huitle, C.A., 2016. Acid blue 29 decolorization and mineralization by anodic oxidation  
1109 with a cold gas spray synthesized Sn-Cu-Sb alloy anode. *Chemosphere* 148, 47-54

1110 dos Santos, A.J., de Lima, M.D., da Silva, D.R., Garcia-Segura, S., Martínez-Huitle, C.A.,  
 1111 2016. Influence of the water hardness on the performance of electro-Fenton approach:  
 1112 Decolorization and mineralization of Eriochrome Black T. *Electrochim. Acta* 208, 156–  
 1113 163.

1114 Drogui, P., Asselin, M., Brar, S.K., Benmoussa, H., Blais, J.F., 2008. Electrochemical  
 1115 removal of pollutants from agro-industry wastewaters. *Sep. Purif. Technol.* 61 (3), 301–  
 1116 310.

1117 El-Desoky, H.S., Ghoneim, M.M., El-Sheikh, R., Zidan, N.M., 2010. Oxidation of levafix CA  
 1118 reactive azo-dyes in industrial wastewater of textile dyeing by electro-generated Fenton's  
 1119 reagent. *J. Hazard. Mater.* 175 (1-3), 858–865.

1120 El-Ghenymy, A., Centellas, F., Rodríguez, R.M., Cabot, P.L., Garrido, J.A., Sirés, I., Brillas,  
 1121 E., 2015. Comparative use of anodic oxidation, electro-Fenton and photoelectro-Fenton  
 1122 with Pt or boron-doped diamond anode to decolorize and mineralize Malachite Green  
 1123 oxalate dye. *Electrochim. Acta* 182, 247–256.

1124 El-Kacemi, S., Zazou, H., Oturan, N., Dietze, M., Hamdani, M., Es-Souni, M., Oturan, M.A.,  
 1125 2017. Nanostructured ZnO-TiO<sub>2</sub> thin film oxide as anode material in electrooxidation of  
 1126 organic pollutants. Application to the removal of dye Amido black 10B from water.  
 1127 *Environ. Sci. Pollut. Res.* 24, 1442-1449.

1128 Eslami, A., Moradi, M., Ghanbari, F., Mehdipour, F., 2013. Decolorization and COD  
 1129 removal from real textile wastewater by chemical and electrochemical Fenton processes: a  
 1130 comparative study. *J. Environ. Health Sci. Eng.* 11, 31.

1131 Faouzi, A.M., Nasr, B., Abdellatif, G., 2007. Electrochemical degradation of anthraquinone  
 1132 dye Alizarin Red S by anodic oxidation on boron-doped diamond. *Dyes Pigments* 73 (1),  
 1133 86-89.

1134 Feng, C., Li, F., Liu, H., Lang, X., Fan, S., 2010a. A dual-chamber microbial fuel cell with  
 1135 conductive film-modified anode and cathode and its application for the neutral electro-  
 1136 Fenton process. *Electrochim. Acta* 55 (6), 2048–2054.

1137 Feng, C-H., Li, F-B., Mai, H-J., Li, X-Z., 2010b. Bio-electro-Fenton process driven by  
 1138 microbial fuel cell for wastewater treatment. *Environ. Sci. Technol.* 44 (5), 1875–1880.

1139 Fernández de Dios, M.Á., González del Campo, A., Fernández, F.J., Rodrigo, M., Pazos, M.,  
 1140 Sanromán, M.Á., 2013. Bacterial–fungal interactions enhance power generation in  
 1141 microbial fuel cells and drive dye decolourisation by an ex situ and in situ electro-Fenton  
 1142 process. *Bioresource Technol.* 148, 39–46.

1143 Flox, C., Arias, C., Brillas, E., Savall, A., Groenen-Serrano, K., 2009. Electrochemical  
 1144 incineration of cresols: a comparative study between PbO<sub>2</sub> and boron-doped diamond  
 1145 anodes. *Chemosphere* 74 (10), 1340–1347.

1146 Flox, C., Cabot, P.L., Centellas, F., Garrido, J.A., Rodríguez, R.M., Arias, C., Brillas, E.,  
 1147 2007a. Solar photoelectro-Fenton degradation of cresols using a flow reactor with a boron-  
 1148 doped diamond anode. *Appl. Catal. B: Environ.* 75 (1-2), 17-28.

1149 Flox, C., Garrido, J.A., Rodríguez, R.M., Cabot, P.L., Centellas, F., Arias, C., Brillas, E.,  
 1150 2007b. Mineralization of herbicide mecoprop by photoelectro-Fenton with UVA and solar  
 1151 light. *Catal. Today* 129 (1-2), 29-36.

1152 Flox, C., Garrido, J.A., Rodríguez, R.M., Centellas, F., Cabot, P.L., Arias, C., Brillas, E.,  
 1153 2005. Degradation of 4,6-dinitro-o-cresol from water by anodic oxidation with a boron-  
 1154 doped diamond electrode. *Electrochim. Acta* 50 (18), 3685–3692.

1155 Fu, F., Wang, Q., Tang, B., 2010a. Effective degradation of CI Acid Red 73 by advanced  
 1156 Fenton process. *J. Hazard. Mater.* 174 (1-3), 17–22.

1157 Fu, L., You, S., Yang, F., Gao, M., Fang, X., Zhang, G., 2010b. Synthesis of hydrogen  
 1158 peroxide in microbial fuel cell. *J. Chem. Technol. Biotechnol.* 85 (5), 715–719.

1159 Ganzenko, O., Trelu, C., Papirio, S., Oturan, N., Huguenot, D., van Hullebusch, E.D.,  
 1160 Esposito, G., Oturan, M.A. (2017). Bioelectro-Fenton: evaluation of a combined  
 1161 biological-advanced oxidation treatment for pharmaceutical wastewater. *Environ. Sci.*  
 1162 *Pollut. Res.* (in press), doi: 10.1007/s11356-017-8450-6.

1163 Garcia-Segura, S., Brillas, E., 2016. Combustion of textile monoazo, diazo and triazo dyes by  
 1164 solar photoelectro-Fenton: Decolorization, kinetics and degradation routes. *Appl. Catal. B:*  
 1165 *Environ.* 181, 681–691

1166 Garcia-Segura, S., El-Ghenymy, A., Centellas, F., Rodríguez, R.M., Arias, C., Garrido, J.A.,  
 1167 Cabot, P.L., Brillas, E., 2012. Comparative degradation of the diazo dye Direct Yellow 4  
 1168 by electro-Fenton, photoelectro-Fenton and photo-assisted electro-Fenton. *J. Electroanal.*  
 1169 *Chem.* 681, 36–43.

1170 Garcia-Segura, S., Salazar, R., Brillas, E., 2013. Mineralization of phthalic acid by solar  
 1171 photoelectro-Fenton with a stirred boron-doped diamond/air-diffusion tank reactor:  
 1172 Influence of  $\text{Fe}^{3+}$  and  $\text{Cu}^{2+}$  catalysts and identification of oxidation products. *Electrochim.*  
 1173 *Acta* 113, 609–619.

1174 George, S.J., Gandhimathi, R., Nidheesh, P.V., Ramesh, S.T., 2013. Oxidation of salicylic  
 1175 acid from aqueous solution with continuous stirred tank reactor by electro-Fenton method.  
 1176 *Environ. Eng. Sci.* 30 (12), 757-764.

1177 George, S.J., Gandhimathi, R., Nidheesh, P.V., Ramesh, S.T., 2014. Electro-Fenton oxidation  
 1178 of salicylic acid from aqueous solution: Batch studies and degradation pathway. *Clean Soil*  
 1179 *Air Water* 42(1), 1701-1711.

1180 George, S.J., Gandhimathi, R., Nidheesh, P.V., Ramesh, S.T., 2016. Optimization of salicylic  
 1181 acid removal by electro Fenton process in a continuous stirred tank reactor using response  
 1182 surface methodology. *Desalination Water Treat.* 57, 4234–4244.

1183 Ghoneim, M.M., El-Desoky, H.S., Zidan, N.M., 2011. Electro-Fenton oxidation of Sunset  
 1184 Yellow FCF azo-dye in aqueous solutions. *Desalination* 274 (1-3), 22–30.

1185 Ghosh, P., Thakur, L.K., Samanta, A.N., Ray, S., 2012. Electro-Fenton treatment of synthetic  
 1186 organic dyes: Influence of operational parameters and kinetic study. *Korean J. Chem. Eng.*  
 1187 29 (9), 1203-1210.

1188 Girish Kumar, S., Gomathi Devi, L., 2011. Review on modified TiO<sub>2</sub> photocatalysis under  
1189 UV/visible light: Selected results and related mechanisms on interfacial charge carrier  
1190 transfer dynamics. *J. Phys. Chem. A* 115 (46), 13211–13241.

1191 Gogate, P.R., Pandit, A.B., 2004. A review of imperative technologies for wastewater  
1192 treatment II: Hybrid methods. *Adv. Environ. Res.* 8 (3-4), 553–597.

1193 Gogate, P.R., Tatake, P.A., Kanthale, P.M., Pandit, A.B., 2002. Mapping of sonochemical  
1194 reactors: Review, analysis, and experimental verification. *AIChE J.* 48 (7), 1542-1560.

1195 Gong, R., Jin, Y., Chen, J., Hu, Y., Sun, J., 2007. Removal of basic dyes from aqueous  
1196 solution by sorption on phosphoric acid modified rice straw. *Dyes Pigments* 73 (3), 332–  
1197 337.

1198 Gong, Y., Radachowsky, S.E., Wolf, M., Nielsen, M.E., Girguis, P.R., Reimers, C.E., 2011.  
1199 Benthic microbial fuel cell as direct power source for an acoustic modem and seawater  
1200 oxygen/temperature sensor system. *Environ. Sci. Technol.* 45 (11), 5047–5053.

1201 Goodridge, F., Scott, K., 1994. *Electrochemical Process Engineering*, Plenum Press, New  
1202 York.

1203 Gözmen, B., Kayan, B., Murat Gizir, A., Hesenov, A., 2009. Oxidative degradations of  
1204 reactive blue 4 dye by different advanced oxidation methods. *J. Hazard. Mater.* 168 (1),  
1205 129–136.

1206 Guivarch, E., Oturan M.A., 2004. The problem of the contamination of waters by synthetic  
1207 dyes: how to destroy them? Application of the electro-Fenton process. *Actual. Chimique*  
1208 277-278, 65-69.

1209 Guivarch, E., Trévin, S., Lahitte, C., Oturan M.A., 2003. Degradation of azo dyes in water by  
1210 electro-Fenton process. *Environ. Chem. Lett.* 1(1), 39-44.

1211 Gupta, N., Oloman, C.W., 2006. Scale-up of the perforated bipole trickle-bed electrochemical  
1212 reactor for the generation of alkaline peroxide. *J. Appl. Electrochem.* 36, 1133–1141.

1213 Haidar, M., Dirany, A., Sirés, I., Oturan, N., Oturan, M.A., 2013. Electrochemical  
1214 degradation of the antibiotic sulfachloropyridazine by hydroxyl radicals generated at a  
1215 BDD anode. *Chemosphere* 91 (9), 1304–1309.

1216 Hammami, S., Oturan, N., Bellakhal, N., Dachraoui, M., Oturan, M.A. 2007. Oxidative  
1217 degradation of direct orange 61 by electro-Fenton process using a carbon felt electrode:  
1218 Application of the experimental design methodology. *J. Electroanal. Chem.* 610 (1), 75–  
1219 84.

1220 Hu, Z., Zhou, M., Zhou, L., Li, Y., Zhang, C. 2014. Effect of matrix on the electrochemical  
1221 characteristics of TiO<sub>2</sub> nanotube arrays based PbO<sub>2</sub> electrode for pollutant degradation.  
1222 *Environ. Sci. Pollut. Res.* 21, 8476–8484.

1223 Iglesias, O., Fernández de Dios, M.A., Pazos, M., Sanromán, M.A., 2013a. Using iron-loaded  
1224 sepiolite obtained by adsorption as a catalyst in the electro-Fenton oxidation of Reactive  
1225 Black 5. *Environ. Sci. Pollut. Res.* 20 (9), 5983-5993.

1226 Iglesias, O., Rosales, E., Pazos, M., Sanromán, M.A., 2013b. Electro-Fenton decolourisation  
1227 of dyes in an airlift continuous reactor using iron alginate beads. *Environ. Sci. Pollut. Res.*  
1228 20 (4), 2252–2261.

1229 Iranifam, M., Zarei, M., Khataee, A.R., 2011. Decolorization of C.I. Basic Yellow 28  
1230 solution using supported ZnO nanoparticles coupled with photoelectro-Fenton process. *J.*  
1231 *Electroanal. Chem.* 659 (1), 107–112.

1232 Isarain-Chávez, E., de la Rosa, C., Martínez-Huitle, C.A., Peralta-Hernández, J.M., 2013. On-  
1233 site hydrogen peroxide production at pilot flow plant: Application to electro-Fenton  
1234 process. *Int. J. Electrochem. Sci.* 8, 3084 – 3094.

1235 Ji, F., Li, C., Zhang, J., Deng, L., 2011. Efficient decolorization of dye pollutants with  
1236  $\text{LiFe}(\text{WO}_4)_2$  as a reusable heterogeneous Fenton-like catalyst. *Desalination* 269 (1-3),  
1237 284–290.

1238 Ju, D.J., Byun, I.G., Park, J.J., Lee, C.H., Ahn, G.H., Park, T.J., 2008. Biosorption of a  
1239 reactive dye (Rhodamine-B) from an aqueous solution using dried biomass of activated  
1240 sludge. *Bioresour. Technol.* 99 (17), 7971–7975.

1241 Jüttner, K., Galla, U., Schmieder, H., 2000. Electrochemical approaches to environmental  
1242 problems in the process industry. *Electrochim. Acta* 45 (15-16), 2575–94.

1243 Karthikeyan, S., Jambulingam, M., Sivakumar, P., Shekhar, A.P., Krithika, J., 2006. Impact  
1244 of textile effluents on fresh water fish *Mastacembelus Armatus* (Cuv.& Val). *E-J. Chem.* 3  
1245 (4), 303-306.

1246 Kavitha, V., Palanivelu, K., 2004. The role of ferrous ion in Fenton and photo-Fenton  
1247 processes for the degradation of phenol. *Chemosphere* 55 (9), 1235–1243

1248 Kayan, B., Gözmen, B., Demirel, M., Murat Gizir, A., 2010. Degradation of acid red 97 dye  
1249 in aqueous medium using wet oxidation and electro-Fenton techniques. *J. Hazard.*  
1250 *Mater.* 177 (1-3), 95–102.

1251 Khataee, A.R., Vahid, B., Behjati, B., Safarpour, M., Joo, S.W., 2014. Kinetic modeling of a  
1252 triarylmethane dye decolorization by photoelectro-Fenton process in a recirculating  
1253 system: Nonlinear regression analysis. *Chem. Eng. Res. Des.* 92 (2), 362–367.

1254 Khataee, A.R., Vatanpour, V., Amani Ghadim, A.R., 2009. Decolorization of C.I. Acid Blue  
1255 9 solution by UV/nano- $\text{TiO}_2$ , Fenton, Fenton-like, electro-Fenton and electrocoagulation  
1256 processes: a comparative study. *J. Hazard. Mater.* 161 (2-3), 1225–1233.

1257 Khataee, A.R., Zarei, M., 2011. Photocatalysis of a dye solution using immobilized ZnO  
1258 nanoparticles combined with photoelectrochemical process. *Desalination* 273 (2-3), 453–  
1259 460.

1260 Khataee, A.R., Zarei, M., Asl, S.K., 2010b. Photocatalytic treatment of a dye solution using  
1261 immobilized  $\text{TiO}_2$  nanoparticles combined with photoelectro-Fenton process:  
1262 Optimization of operational parameters. *J. Electroanal. Chem.* 648 (2), 143–150.

- 1263 Khataee, A.R., Zarei, M., Moradkhannejhad, L., 2010a. Application of response surface  
1264 methodology for optimization of azo dye removal by oxalate catalyzed photoelectro-  
1265 Fenton process using carbon nanotube-PTFE cathode. *Desalination* 258 (1-3), 112–119.
- 1266 Klemola, K., Honkalampi-Hämäläinen, U., Liesivuori, J., Pearson, J., Lindström-Seppä, P.,  
1267 2006. Evaluating the toxicity of reactive dyes and fabrics with the spermatozoa motility  
1268 inhibition test. *Autex Res. J.* 6 (3), 182-190.
- 1269 Klemola, K., Pearson, J., Lindstrom-Seppä, P., 2007. Evaluating the toxicity of reactive dyes  
1270 and dyed fabrics with the HaCaT cytotoxicity test. *Autex Res. J.* 7 (3), 217-223.
- 1271 Kwon, B.G., Lee, D.S., Kang, N., Yoon, J., 1999. Characteristics of p-chlorophenol oxidation  
1272 by Fenton's reagent. *Water Res.* 33 (9), 2110-2118.
- 1273 Labiadh, L., Oturan, M.A., Panizza, M., Ben Hamadi, N., Ammar, S., 2015. Complete  
1274 removal of AHPS synthetic dye from water using new electro-Fenton oxidation catalyzed  
1275 by natural pyrite as heterogeneous catalyst. *J. Hazard. Mater.* 297, 34-41
- 1276 Labiadh, L., Barbucci, A., Carpanese, M.P., Gadri, A., Ammar, S., Panizza, M., 2016.  
1277 Comparative depollution of Methyl Orange aqueous solutions by electrochemical  
1278 incineration using TiRuSnO<sub>2</sub>, BDD and PbO<sub>2</sub> as high oxidation power anodes. *J.*  
1279 *Electroanal. Chem.* 766, 94–99.
- 1280 Lahkimi, A., Oturan, M.A., Oturan, N., Chaouch, M., 2007. Removal of textile dyes from  
1281 water by the electro-Fenton process. *Environ. Chem. Lett.* 5, 35–39.
- 1282 Lam, S-M., Sin, J-C., Abdullah, A.Z., Mohamed, A.R., 2012. Degradation of wastewaters  
1283 containing organic dyes photocatalysed by zinc oxide: A review. *Desalination Water*  
1284 *Treat.* 41 (1-3), 131–169.
- 1285 Le, T.X.H., Bechelany, M., Lacour, S., Oturan, N., Oturan, M.A., Cretin, M., 2015. High  
1286 removal efficiency of dye pollutants by electron-Fenton process using a graphene based  
1287 cathode. *Carbon* 94, 1003–1011
- 1288 Le, T.X.H., Nguyen, T.V., Yacouba, Z.A., Zoungrana, L., Avril, F., Petit, E., Mendret, J.,  
1289 Bonniol, V., Bechelany, M., Lacour, S., Lesage, G., Cretin, M., 2016. Toxicity removal  
1290 assessments related to degradation pathways of azo dyes: Toward an optimization of  
1291 Electro-Fenton treatment. *Chemosphere* 161, 308-318
- 1292 Li, H., Lei, H., Yu, Q., Li, Z., Feng, X., Yang, B., 2010b. Effect of low frequency ultrasonic  
1293 irradiation on the sonoelectro-Fenton degradation of cationic red X-GRL. *Chem. Eng. J.*  
1294 160 (2), 417–422.
- 1295 Li, H., Zhu, X., Ni, J., 2010a. Inactivation of *Escherichia coli* in Na<sub>2</sub>SO<sub>4</sub> electrolyte using  
1296 boron-doped diamond anode. *Electrochim. Acta* 56 (1), 448–453.
- 1297 Liang, L., An, Y.R., Yu, F.K., Liu, M.M, Ren, G.B., Zhou, M.H. 2016. Novel rolling-made  
1298 gas-diffusion electrode loading trace transition metal for efficient heterogeneous electro-  
1299 Fenton-like. *J. Environ. Chem. Eng.* 4, 4400-4408.

1300 Lin, H., Zhang, H., Wang, X., Wang, L., Wu, J., 2014. Electro-Fenton removal of Orange II  
1301 in a divided cell: Reaction mechanism, degradation pathway and toxicity evolution. *Sep.*  
1302 *Purif. Technol.* 122, 533–540.

1303 Liu, X-W., Sun, X-F., Li, D-B., Li, W-W., Huang, Y-X., Sheng, G-P., Yu, H-Q., 2012.  
1304 Anodic Fenton process assisted by a microbial fuel cell for enhanced degradation of  
1305 organic pollutants. *Water Res.* 46 (14), 4371-4378.

1306 Lounis, M., Samar, M.E., Hamdaoui, O., 2016. Sono-electrochemical degradation of Orange  
1307 G in pure water, natural water, and seawater: effect of operating parameters. *Desalination*  
1308 *Water Treat.* 57(47), 22533-22542

1309 Ma, L., Zhou, M.H., Ren, G.B., Yang, W.L., Liang, L., 2016. A highly energy-efficient flow-  
1310 through electro-Fenton process for organic pollutants degradation. *Electrochim. Acta* 200,  
1311 222-230

1312 Magario, I., García Einschlag, F.S., Rueda, E.H., Zygadlo, J., Ferreira, M.L., 2012.  
1313 Mechanisms of radical generation in the removal of phenolderivatives and pigments using  
1314 different Fe-based catalytic systems. *J. Mol. Catal. A: Chem.* 352, 1-20.

1315 Malik, P.K., 2003. Use of activated carbons prepared from sawdust and rice-husk for  
1316 adsorption of acid dyes: a case study of Acid Yellow 36. *Dyes Pigments* 56 (3), 239–249.

1317 Mane, V.S., Mall, I.D., Srivastava, V.C., 2007. Use of bagasse fly ash as an adsorbent for the  
1318 removal of brilliant green dye from aqueous solution. *Dyes Pigments* 73 (3), 269–278.

1319 Martínez, S.S., Uribe, E.V., 2012. Enhanced sonochemical degradation of azure B dye by the  
1320 electroFenton process. *Ultrason.Sonochem.* 19 (1), 174–178.

1321 Martínez-Huitle, C.A., Brillas, E., 2009. Decontamination of wastewaters containing synthetic  
1322 organic dyes by electrochemical methods: A general review. *Appl. Catal. B: Environ.* 87  
1323 (3-4), 105–145.

1324 Martínez-Huitle, C.A., dos Santos, E.V., de Araújo, D.M., Panizza, M., 2012. Applicability  
1325 of diamond electrode/anode to the electrochemical treatment of areal textile effluent. *J.*  
1326 *Electroanal. Chem.* 674, 103–107.

1327 Mathur, N., Bhatnagar, P., Bakre, P., 2005. Assessing mutagenicity of textile dyes from pali  
1328 (Rajasthan) using ames bioassay. *Appl. Ecology Environ. Res.* 4 (1), 111–118.

1329 Medvedev, Z.A., Crowne, H.M., Medvedeva, M.N., 1988. Age related variations of hepato  
1330 carcinogenic effect of azo dye (3'-MDAB) as linked to the level of hepatocyte  
1331 polyploidization. *Mech. Ageing Dev.* 46 (1-3), 159-174.

1332 Migliorini, F.L., Braga, N.A., Alves, S.A., Lanza, M.R.V., Baldan, M.R., Ferreira, N.G.,  
1333 2011. Anodic oxidation of wastewater containing the Reactive Orange 16 Dye using  
1334 heavily boron-doped diamond electrodes. *J. Hazard. Mater.* 192 (3), 1683–1689.

1335 Miled, W., Said, A., Roudseli, S., 2010. Decolorization of high polluted textile wastewater by  
1336 indirect electrochemical oxidation process. *JTATM* 6 (3), 1-6.

1337 Moreira, F.C., Garcia-Segura, S., Vilar, V.J.P., Boaventura, R.A.R., Brillas, E., 2013.  
 1338 Decolorization and mineralization of Sunset Yellow FCF azo dye by anodic oxidation,  
 1339 electro-Fenton, UVA photoelectro-Fenton and solar photoelectro-Fenton processes. *Appl.*  
 1340 *Catal. B: Environ.* 142, 877-890.

1341 Murati, M., Oturan, N., Aaron, J-J., Dirany, A., Tassin, B., Zdravkovski, Z., Oturan, M.A.,  
 1342 2012. Degradation and mineralization of sulcotrione and mesotrione in aqueous medium  
 1343 by the electro-Fenton process: a kinetic study. *Environ. Sci. Pollut. Res.* 19 (5), 1563–  
 1344 1573.

1345 Muruganandham, M., Swaminathan, M., 2004. Decolourisation of Reactive Orange 4 by  
 1346 Fenton and photo-Fenton oxidation technology. *Dyes Pigments* 63 (3), 315-321

1347 Murugananthan, M., Yoshihara, S., Rakuma, T., Uehara, N., Shirakashi, T., 2007.  
 1348 Electrochemical degradation of 17 $\beta$ -estradiol (E2) at boron-doped diamond (Si/BDD) thin  
 1349 film electrode. *Electrochim. Acta* 52 (9), 3242–3249.

1350 Namasivayam, C., Kavitha, D., 2002. Removal of Congo Red from water by adsorption onto  
 1351 activated carbon prepared from coir pith, an agricultural solid waste. *Dyes Pigments* 54  
 1352 (1), 47–58.

1353 Nava, J.L., Quiroz, M.A., Martínez-Huitle, C.A., 2008. Electrochemical treatment of  
 1354 synthetic wastewaters containing alphazurine A dye: Role of Electrode material in the  
 1355 colour and cod removal. *J. Mex. Chem. Soc.* 52 (4), 249-255.

1356 Neyens, E., Baeyens, J., 2003. A review of classic Fenton's peroxidation as an advanced  
 1357 oxidation technique. *J. Hazard. Mater.* B98 (1-3), 33–50.

1358 Nidheesh, P.V., 2015. Heterogeneous Fenton catalysts for the abatement of organic pollutants  
 1359 from aqueous solution: a review. *RSC Adv.* 5, 40552–40577.

1360 Nidheesh, P.V., Gandhimathi, R., 2012. Trends in electro-Fenton process for water and  
 1361 wastewater treatment: An overview. *Desalination* 299, 1–15.

1362 Nidheesh, P.V., Gandhimathi, R., 2014a. Removal of rhodamine B from aqueous solution  
 1363 using graphite- graphite electro Fenton system. *Desalination Water Treat.* 52, 1872–1877.

1364 Nidheesh, P.V., Gandhimathi, R., 2014b. Comparative removal of rhodamine B from aqueous  
 1365 solution by electro Fenton and electro Fenton like processes. *Clean- Soil, Air, Water.*  
 1366 42(6), 779-784.

1367 Nidheesh, P.V., Gandhimathi, R., 2014c. Effect of solution pH on the performance of three  
 1368 electrolytic advanced oxidation processes for the treatment of textile wastewater and  
 1369 sludge characteristics. *RSC Adv.* 4, 27946–27954.

1370 Nidheesh, P.V., Gandhimathi, R., 2014d. Electrolytic removal of Rhodamine B from aqueous  
 1371 solution by peroxicoagulation process. *Environ. Sci. Pollut. Res.* 21, 8585–8594.

1372 Nidheesh, P.V., Gandhimathi, R., 2015a. Electro Fenton oxidation for the removal of  
 1373 Rhodamine B from aqueous solution in a bubble column reactor under continuous mode.  
 1374 *Desalination Water Treat.* 55, 263-273.

1375 Nidheesh, P.V., Gandhimathi, R., 2015b. Textile Wastewater Treatment by Electro-Fenton  
1376 Process in Batch and Continuous Modes. *J. Hazard. Toxic Radioact. Waste* 19(3),  
1377 04014038.

1378 Nidheesh, P.V., Gandhimathi, R., Ramesh, S.T., 2013. Degradation of dyes from aqueous  
1379 solution by Fenton processes: A Review. *Environ. Sci. Pollut. Res.* 20, 2099–2132.

1380 Nidheesh, P.V., Gandhimathi, R., Sanjini, N.S., 2014b.  $\text{NaHCO}_3$  enhanced Rhodamine B  
1381 removal from aqueous solution by graphite–graphite electro Fenton system. *Sep. Purif.*  
1382 *Technol.* 132, 568-576.

1383 Nidheesh, P.V., Gandhimathi, R., Velmathi, S., Sanjini, N.S., 2014a. Magnetite as a  
1384 heterogeneous electro Fenton catalyst for the removal of Rhodamine B from aqueous  
1385 solution. *RSC Adv.* 4, 5698-5708.

1386 Olvera-Vargas, H., Cocerva, T., Oturan, N., Buisson, D., Oturan, M.A., 2016a. Bioelectro-  
1387 Fenton: A sustainable integrated process for removal of organic pollutants from water:  
1388 Application to mineralization of metoprolol. *Journal of Hazardous Materials* 319 (2016)  
1389 13–23.

1390 Olvera-Vargas, H., Oturan, N., Buisson, D., Oturan, M.A., 2016b. A coupled Bio-EF process  
1391 for mineralization of the pharmaceuticals Furosemide and Ranitidine: feasibility  
1392 assessment. *Chemosphere*, 155, 606-613.

1393 Olvera-Vargas, H., Oturan, N., Aravindakumar, C.T., Sunil Paul, M.M., Sharma, V.K.,  
1394 Oturan, M.A., 2014. Electro-oxidation of the dye azure B: kinetics, mechanism, and by-  
1395 products. *Environ. Sci. Pollut. Res.* 21, 8379-8386.

1396 Oturan, M.A. Pinson, J., 1995. Hydroxylation by electrochemically generated  $\bullet\text{OH}$  radicals.  
1397 Mono- and polyhydroxylation of benzoic acid: products and isomers' distribution. *J. Phys.*  
1398 *Chem.* 99(38), 13948-13954.

1399 Oturan, M.A., 2000. An ecologically effective water treatment technique using  
1400 electrochemically generated hydroxyl radicals for in situ destruction of organic pollutants:  
1401 Application to herbicide 2,4-D. *J. Appl. Electrochem.* 30, 475-482.

1402 Oturan, M.A., Aaron, J.-J., 2014. Advanced oxidation processes in water/wastewater  
1403 treatment: Principles and applications. A review. *Crit. Rev. Env. Sci. Technol.* 44, 2577-  
1404 2641.

1405 Oturan, M.A., Edelahe, M.C., Oturan, N., El Kacemi, K., Aaron, J.-J., 2010a. Kinetics of  
1406 oxidative degradation/mineralization pathways of the phenylurea herbicides diuron,  
1407 monuron and fenuron in water during application of the electro-Fenton process. *Appl.*  
1408 *Catal. B: Environ.* 97 (1-2), 82–89.

1409 Oturan, M.A., Guivarch, E., Oturan, N., Sirés, I., 2008a. Oxidation pathways of malachite  
1410 green by  $\text{Fe}^{3+}$ -catalyzed electro-Fenton process. *Appl. Catal. B: Environ.* 82 (3-4), 244–  
1411 254.

- 1412 Oturan, M.A., Oturan, N., Lahitte, C., Trevin, S., 2001. Production of hydroxyl radicals by  
1413 electrochemically assisted Fenton's reagent. Application to the mineralization of an  
1414 organic micropollutant, the pentachlorophenol. *J. Electroanal. Chem.*, 507 (1-2), 96-102.
- 1415 Oturan, M.A., Peirotten, J., Chartrin, P., Acher, A.J., 2000. Complete destruction of p-  
1416 Nitrophenol in aqueous medium by electro-Fenton method. *Environ. Sci. Technol.* 34  
1417 (16), 3474-3479.
- 1418 Oturan, M.A., Sirés, I., Oturan, N., Pérocheau, S., Laborde, J-L., Trévin, S., 2008b.  
1419 Sonoelectro-Fenton process: A novel hybrid technique for the destruction of organic  
1420 pollutants in water. *J. Electroanal. Chem.* 624 (1-2), 329-332.
- 1421 Oturan, M.A., Oturan, N., Aaron, J.-J., 2004. Treatment of organic micropollutants in aqueous  
1422 medium by advanced oxidation process. *Actual. Chimique* 277-278, 57-64
- 1423 Oturan, N., Brillas, E., Oturan, M.A., 2012. Unprecedented total mineralization of atrazine  
1424 and cyanuric acid by anodic oxidation and electro-Fenton with a boron-doped diamond  
1425 anode. *Environ. Chem. Lett.*, 10(2), 165-170.
- 1426 Oturan, N., Zhou, M., Oturan, M.A., 2010b. Metomyl Degradation by electro-Fenton and  
1427 electro-Fenton-like processes: A kinetics study of the effect of the nature and  
1428 concentration of some transition metal ions as catalyst. *J. Phys. Chem. A* 114 (39), 10605-  
1429 10611.
- 1430 Özcan, A., Oturan, M.A., Oturan, N., Sahin, Y., 2009b. Removal of Acid Orange 7 from  
1431 water by electrochemically generated Fenton's reagent. *J. Hazard. Mater.* 163 (2-3), 1213-  
1432 1220.
- 1433 Özcan, A., Sahin, Y., Oturan, M.A., 2008b. Removal of prophan from water by using  
1434 electro-Fenton technology: Kinetics and mechanism. *Chemosphere* 73 (5), 737-744.
- 1435 Özcan, A., Sahin, Y., Oturan, M.A., 2013. Complete removal of the insecticide azinphos  
1436 methyl from water by the electro-Fenton method A kinetic and mechanistic study. *Water*  
1437 *Res.* 47 (3), 1470-1479.
- 1438 Özcan, A., Sahin, Y., Koparal, A.S., Oturan, M.A., 2008a. Prophan mineralization in  
1439 aqueous medium by anodic oxidation using boron-doped diamond anode: Influence of  
1440 experimental parameters on degradation kinetics and mineralization efficiency. *Water Res.*  
1441 42 (12), 2889-2898.
- 1442 Özcan, A., Sahin, Y., Koparal, A.S., Oturan, M.A., 2009a. A comparative study on the  
1443 efficiency of electro-Fenton process in the removal of prophan from water. *Appl. Catal.*  
1444 *B: Environ.* 89 (3-4), 620-626.
- 1445 Özcan, A., Sahin, Y., Koparal A.S., Oturan, M.A., 2008c. Carbon sponge as a new cathode  
1446 material for the electro-Fenton process: Comparison with carbon felt cathode and  
1447 application to degradation of synthetic dye basic blue 3 in aqueous medium. *J. Electroanal.*  
1448 *Chem.* 616 (1-2), 71-78.

1449 Panizza, M., Barbucci, A., Ricotti, R., Cerisola, G., 2007. Electrochemical degradation of  
1450 methylene blue. *Sep. Purif. Technol.* 54, 382–387.

1451 Panizza, M., Cerisola, G., 2001. Removal of organic pollutants from industrial wastewater by  
1452 electrogenerated Fenton's reagent. *Water Res.* 35 (16), 3987–3992.

1453 Panizza, M., Cerisola, G., 2008. Electrochemical degradation of methyl red using BDD and  
1454  $\text{PbO}_2$  anodes. *Ind. Eng. Chem. Res.* 47 (18), 6816–6820.

1455 Panizza, M., Cerisola, G., 2009. Direct and mediated anodic oxidation of organic pollutants.  
1456 *Chem. Rev.*, 109 (2009) 6541–6569.

1457 Panizza, M., Oturan, M.A., 2011. Degradation of Alizarin Red by electro-Fenton process  
1458 using a graphite-felt cathode. *Electrochim. Acta* 56 (20), 7084–7087.

1459 Peralta-Hernández, J.M., Martínez-Huitile, C.A., Guzmán-Mar, J.L., Hernández-Ramírez, A.,  
1460 2009. Recent advances in the application of electro-Fenton and photoelectro-Fenton  
1461 process for removal of synthetic dyes in wastewater treatment. *J. Environ. Eng. Manage.*  
1462 19 (5), 257–265.

1463 Peralta-Hernández, J.M., Meas-Vong, Y., Rodríguez, F.J., Chapman, T.W., Maldonado, M.I.,  
1464 Godínez, L.A., 2008. Comparison of hydrogen peroxide-based processes for treating dye-  
1465 containing wastewater: Decolorization and destruction of Orange II azo dye in dilute  
1466 solution. *Dyes Pigments* 76 (3), 656–662.

1467 Percy, A.J., Moore, N., Chipman, J.K., 1989. Formation of nuclear anomalies in rat intestine  
1468 by benzidine and its biliary metabolites. *Toxicol.* 57 (2), 217–223.

1469 Petrucci, E., Montanaro, D., 2011. Anodic oxidation of a simulated effluent containing  
1470 Reactive Blue 19 on a boron-doped diamond electrode. *Chem. Eng. J.* 174 (2-3), 612–618.

1471 Pignatello, J.J.; Oliveros, E., Mackay, A., 2006. Advanced oxidation processes for organic  
1472 contaminant destruction based on the Fenton reaction and related chemistry. *Crit. Rev.*  
1473 *Environ. Sci. Technol.* 36 (1), 1–84.

1474 Ponnusami, V., Vikram, S., Srivastava, S.N., 2008. Guava (*Psidium guajava*) leaf powder:  
1475 Novel adsorbent for removal of methylene blue from aqueous solutions. *J. Hazard.*  
1476 *Mater.* 152 (1), 276–286.

1477 Pradhan, A.A., Gogate, P.R., 2010. Degradation of p-nitrophenol using acoustic cavitation  
1478 and Fenton chemistry. *J. Hazard. Mater.* 173 (1-3), 517–522.

1479 Rabaey, K., Rozendal, R.A., 2010. Microbial electrosynthesis- revisiting the electrical route  
1480 for microbial production. *Nature Rev. Microbiol.* 8, 706–716.

1481 Ramachandran, R., Saraswathi, R., 2011. Sonoelectrochemical studies on mass transport in  
1482 some standard redox systems. *Russ. J. Electrochem.* 47 (1), 15–25.

1483 Ramírez, C., Saldana, A., Hernández, B., Acero, R., Guerra, R., Garcia-Segura, S., Brillas, E.,  
1484 Peralta-Hernández, J.M., 2013. Electrochemical oxidation of methyl orange azo dye at  
1485 pilot flow plant using BDD technology. *J. Ind. Eng. Chem.* 19 (2), 571–579.

1486 Rauf, M.A., Meetani, M.A., Hisaindee, S., 2011. An overview on the photocatalytic  
1487 degradation of azo dyes in the presence of TiO<sub>2</sub> doped with selective transition metals.  
1488 Desalination 276 (1-3), 13–27.

1489 Ren, G.B., Zhou, M.H., Liu, M.M., Ma, L., Yang, H.J., 2016. A novel vertical-flow electro-  
1490 Fenton reactor for organic wastewater treatment. Chem. Eng. J. 298, 55-67.

1491 Rodriguez, J., Rodrigo, M.A., Panizza, M., Cerisola, G., 2009. Electrochemical oxidation of  
1492 Acid Yellow 1 using diamond anode. J. Appl. Electrochem. 39 (11), 2285-2289.

1493 Rosales, E., Iglesias, O., Pazos, M., Sanromán, M.A., 2012. Decolourisation of dyes under  
1494 electro-Fenton process using Fe alginate gel beads. J. Hazard. Mater. 213–214, 369–377.

1495 Roshini, P.S., Gandhimathi, R., Ramesh, S.T., Nidheesh, P.V., 2018. Combined electro-  
1496 Fenton and biological processes for the treatment of industrial textile effluent:  
1497 Mineralization and toxicity analysis. J. Hazard. Toxic Radioact. Waste 21(4), doi:  
1498 10.1061/(ASCE)HZ.2153-5515.0000370

1499 Ruiz, E.J., Arias, C., Brillas, E., Hernández-Ramírez, A., Peralta-Hernández, J.M., 2011b.  
1500 Mineralization of Acid Yellow 36 azo dye by electro-Fenton and solar photoelectro-  
1501 Fenton processes with a boron-doped diamond anode. Chemosphere 82 (4), 495–501.

1502 Ruiz, E.J., Hernández-Ramírez, A., Peralta-Hernández, J.M., Arias, C., Brillas, E., 2011a.  
1503 Application of solar photoelectro-Fenton technology to azo dyes mineralization: Effect of  
1504 current density, Fe<sup>2+</sup> and dye concentrations. Chem. Eng. J. 171 (2), 385–392.

1505 Saez, C., Panizza, M., Rodrigo, M.A., Cerisola, G., 2007. Electrochemical incineration of  
1506 dyes using a boron-doped diamond anode. J. Chem. Technol. Biot. 82 (6), 575-581.

1507 Şahinkaya, S., 2013. COD and color removal from synthetic textile wastewater by ultrasound  
1508 assisted electro-Fenton oxidation process. J. Ind. Eng. Chem. 19 (2), 601–605.

1509 Salari, D., Niaei, A., Khataee A., Zarei, M., 2009. Electrochemical treatment of dye solution  
1510 containing C.I. basic yellow 2 by the peroxi-coagulation method and modeling of  
1511 experimental results by artificial neural networks. J. Electroanal. Chem. 629 (1-2), 117–  
1512 125.

1513 Salazar, R., Garcia-Segura, S., Ureta-Zañartu, M.S., Brillas, E., 2011. Degradation of  
1514 disperse azo dyes from water by solar photoelectro-Fenton. Electrochim. Acta 56 (18),  
1515 6371–6379.

1516 Salazar, R., Ureta-Zañartu, M.S., 2012. Degradation of acid violet 7 and reactive black 5 in  
1517 water by electro-Fenton and photo electro-Fenton. J. Chil. Chem. Soc. 57 (1), 999-1003.

1518 Saltmiras, D.A., Lemley, A.T., 2000. Degradation of ethylene thiourea (ETU) with three  
1519 Fenton treatment processes. J. Agric. Food Chem. 48 (12), 6149–6157.

1520 Sandhya, S., Sarayu, K., Swaminathan, K., 2008. Determination of kinetic constants of hybrid  
1521 textile wastewater treatment system. Bioresource Technol. 99 (13), 5793–5797.

- Scialdone, O., 2009. Electrochemical oxidation of organic pollutants in water at metal oxide electrodes: A simple theoretical model including direct and indirect oxidation processes at the anodic surface. *Electrochim. Acta* 54 (26), 6140–6147.
- Scialdone, O., Galia, A., Sabatino, S., 2013. Electro-generation of H<sub>2</sub>O<sub>2</sub> and abatement of organic pollutant in water by an electro-Fenton process in a microfluidic reactor. *Electrochem. Commun.* 26, 45–47.
- Sekar, P., Hari Prasad, S., Decca Raman, M., 2009. Effect of textile dye industry effluent on the nutritive value of fresh water female crab *Spiralothelphusa hydrodroma* (Herbst). *J. Appl. Sci. Res.* 5 (11), 2041-2048.
- Siddique, M., Farooq, R., Khan, Z.M., Khan, Z., Shaukat, S.F., 2011. Enhanced decomposition of reactive blue 19 dye in ultrasound assisted electrochemical reactor. *Ultrason. Sonochem.* 18 (1), 190–196.
- Sirés, I., Brillas, E., Oturan, M.A., Rodrigo, M.A., Panizza, M., 2014. Electrochemical advanced oxidation processes: today and tomorrow. A review. *Environ. Sci. Pollut. Res.* 21, 8336-8367.
- Sirés, I., Cabot, P.L., Centellas, F., Garrido, J.A., Rodríguez, R.M., Arias, C., Brillas, E., 2006. Electrochemical degradation of clofibric acid in water by anodic oxidation Comparative study with platinum and boron-doped diamond electrodes. *Electrochim. Acta* 52 (1), 75–85.
- Sirés, I., Guivarch, E., Oturan, N., Oturan, M.A., 2008. Efficient removal of triphenylmethane dyes from aqueous medium by in situ electrogenerated Fenton's reagent at carbon-felt cathode. *Chemosphere* 72 (4), 592–600.
- Sivasankar, T., Moholkar, V.S., 2010. Physical insight into the sonochemical degradation of 2,4-dichlorophenol. *Environ. Technol.* 31 (14), 1483–1494.
- Solano, A.M.S., Garcia-Segura, S., Martínez-Huitle, C.A., Brillas, E., 2015. Degradation of acidic aqueous solutions of the diazo dye Congo Red by photo-assisted electrochemical processes based on Fenton's reaction chemistry. *Appl. Catal. B: Environ.* 168-169, 559–571
- Song, S., Fan, J., He, Z., Zhan, L., Liu, Z., Chen, J., Xu, X., 2010. Electrochemical degradation of azo dye C.I. Reactive Red 195 by anodic oxidation on Ti/SnO<sub>2</sub>–Sb/PbO<sub>2</sub> electrodes. *Electrochim. Acta* 55 (11), 3606–3613.
- Sopaj F., Rodrigo M.A., Oturan N., Podvorica F.I., Pinson J., Oturan M.A., 2015. Influence of the anode materials on the electrochemical oxidation efficiency. Application to oxidative degradation of the pharmaceutical amoxicillin. *Chem. Eng. J.* 262, 286–294.
- Sopaj F., Oturan N., Pinson J., Podvorica F., Oturan M.A., 2016. Effect of the anode materials on the efficiency of the electro-Fenton process for the mineralization of the antibiotic sulfamethazine. *Appl. Catal. B: Environ.* 199, 331-341.
- Srivastava, S., Sinha, R., Roy, D., 2004. Toxicological effects of malachite green. *Aquat. Toxicol.* 66 (3), 319-329.

1561 Sun, J., Lu, H., Du, L., Lin, H., Li, H., 2011. Anodic oxidation of anthraquinone dye Alizarin  
1562 Red S at Ti/BDD electrodes. *Appl. Surf. Sci.* 257 (15), 6667–6671.

1563 Sun, S.P., Li, C.J., Sun, J.H., Shi, S.H., Fan, M.H., Zhou, Q., 2009. Decolorization of an azo  
1564 dye Orange G in aqueous solution by Fenton oxidation process: Effect of system  
1565 parameters and kinetic study. *J. Hazard. Mater.* 161 (2-3), 1052-1057.

1566 Suslick, K.S., 1989. The chemical effects of ultrasound. *Sci. Am.* 260, 80-87.

1567 Suteu, D., Bilba, D., 2005. Equilibrium and kinetic study of reactive dye brilliant red HE-3B  
1568 adsorption by activated charcoal. *Acta Chim. Slov.* 52, 73–79.

1569 Tang, W.Z., Huang, C.P., 1996. 2,4-dichlorophenol oxidation kinetics by Fenton's reagent.  
1570 *Environ. Technol.* 17 (12), 1371-1378.

1571 Umbuzeiro, G.A., Freeman, H., Warren, S.H., Kummrow, F., Claxton, L.D., 2005.  
1572 Mutagenicity evaluation of the commercial product CI Disperse Blue 291 using different  
1573 protocols of the Salmonella assay. *Food Chem. Toxicol.* 43 (1), 49-56.

1574 Vasudevan, S., Oturan, M.A., 2014. Electrochemistry as cause and cure in water pollution.  
1575 An Overview. *Environ. Chem. Lett.* 12(1), 97-108.

1576 Venu, D., Gandhimathi, R., Nidheesh, P.V., Ramesh, S.T., 2014. Treatment of stabilized  
1577 landfill leachate using peroxicoagulation process. *Sep. Purif. Technol.* 129, 64–70.

1578 Venu, D., Gandhimathi, R., Nidheesh, P.V., Ramesh, S.T., 2016. Effect of solution pH on  
1579 leachate treatment mechanism of peroxicoagulation process. *J. Hazard. Toxic Radioact.*  
1580 *Waste* 20 (3), 06016001.

1581 Wang, A., Qu, J., Liu, H., Ru, J., 2008b. Mineralization of an azo dye Acid Red 14 by  
1582 photoelectro-Fenton process using an activated carbon fiber cathode. *Appl. Catal. B:*  
1583 *Environ.* 84 (3-4), 393–399.

1584 Wang, C.T., Chou, W.L., Chung, M.H., Kuo, Y.M., 2010. COD removal from real dyeing  
1585 wastewater by electro-Fenton technology using an activated carbon fiber cathode.  
1586 *Desalination* 253 (1-3), 129–134.

1587 Wang, C-T., Hu, J-L., Chou, W-L., Kuo, Y-M., 2008a. Removal of color from real dyeing  
1588 wastewater by Electro-Fenton technology using a three-dimensional graphite cathode. *J.*  
1589 *Hazard. Mater.* 152 (2), 601–606.

1590 Wang, Q., Jin, T., Hu, Z.X., Zhou, L., Zhou, M.H., 2013. TiO<sub>2</sub>-NTs/SnO<sub>2</sub>-Sb anode for  
1591 efficient electrocatalytic degradation of organic pollutants: Effect of TiO<sub>2</sub>-NTs  
1592 architecture. *Sep. Purif. Technol.* 102, 180-186.

1593 Wang, Q., Lemley, A.T., 2002. Oxidation of diazinon by anodic Fenton treatment. *Water*  
1594 *Res.* 36 (13), 3237–3244.

1595 Wang, Q., Lemley, A.T., 2003. Oxidative degradation and detoxification of aqueous  
1596 carbofuran by membrane anodic Fenton treatment. *J. Hazard. Mater.* B98 (1-3), 241–255.

1597 Wang, Z., Qi, J., Feng, Y., Li, K., Li, X., 2014a. Fabrication and electrocatalytic performance  
1598 of a novel particle electrode. *Catal. Commun.* 46, 165–168.

1599 Wang, Z., Qi, J., Feng, Y., Li, K., Li, X., 2014b. Preparation of catalytic particle electrodes  
1600 from steel slag and its performance in a three-dimensional electrochemical oxidation  
1601 system. *J. Ind. Eng. Chem.* 20(5), 3672-3677

1602 Wells, C.F., Salam, M.A., 1965. Hydrolysis of ferrous ions: A kinetic method for  
1603 determination of the Fe(II) species. *Nature* 205, 690–692.

1604 Wells, C.F., Salam, M.A., 1968. The effect of pH on the kinetics of the reaction of iron(II)  
1605 with hydrogen peroxide in perchlorate media. *J. Chem. Soc. A* 1968, 24–29.

1606 Xu, X., Chen, J., Zhang, G., Song, Y., Yang, F., 2014. Homogeneous electro-Fenton  
1607 oxidative degradation of reactive brilliant blue using a graphene doped gas-diffusion  
1608 cathode. *Int. J. Electrochem. Sci.* 9, 569–579.

1609 Yang, W., Zhou, M.H., Cai, J. J., Liang, L., Ren, G.B., 2017. Ultrahigh yield of hydrogen  
1610 peroxide on graphite felt cathode modified with electrochemically exfoliated graphene. *J.*  
1611 *Mater. Chem. A* 5, 8070–8080.

1612 Yao, Y., Zhao, C., Zhao, M., Wang, X., 2013. Electrocatalytic degradation of methylene blue  
1613 on PbO<sub>2</sub>-ZrO<sub>2</sub> nanocomposite electrodes prepared by pulse electrodeposition. *J. Hazard.*  
1614 *Mater.* 263 (2), 726–734.

1615 Yavuz, Y., Shahbazi, R., 2012. Anodic oxidation of Reactive Black 5 dye using boron doped  
1616 diamond anodes in a bipolar trickle tower reactor. *Sep. Purif. Technol.* 85, 130–136.

1617 Yu, F.K., Zhou, M.H., Yu, X.M. 2015. Cost-effective electro-Fenton using modified graphite  
1618 felt that dramatically enhanced on H<sub>2</sub>O<sub>2</sub> electro-generation without external aeration.  
1619 *Electrochim. Acta* 163, 182-189.

1620 Yue, L., Wang, K., Guo, J., Yang, J., Luo, X., Lian, J., Wang, L., 2014. Enhanced  
1621 electrochemical oxidation of dye wastewater with Fe<sub>2</sub>O<sub>3</sub> supported catalyst. *J. Ind. Eng.*  
1622 *Chem.* 20 (2), 725–731.

1623 Zarei, M., Khataee, A.R., Ordikhani-Seyedlar, R., Fathinia, M., 2010b. Photoelectro-Fenton  
1624 combined with photocatalytic process for degradation of an azo dye using supported TiO<sub>2</sub>  
1625 nanoparticles and carbon nanotube cathode: Neural network modeling. *Electrochim. Acta*  
1626 55 (24), 7259–7265.

1627 Zarei, M., Niaei, A., Salari, D., Khataee, A., 2010a. Removal of four dyes from aqueous  
1628 medium by the peroxi-coagulation method using carbon nanotube-PTFE cathode and  
1629 neural network modeling. *J. Electroanal. Chem.* 639 (1-2), 167–174.

1630 Zarei, M., Salari, D., Niaei, A., Khataee, A., 2009. Peroxi-coagulation degradation of C.I.  
1631 basic yellow 2 based on carbon-PTFE and carbon nanotube-PTFE electrodes as cathode.  
1632 *Electrochim. Acta* 54 (26), 6651–6660.

1633 Zhang, C., Jiang, Y., Li, Y., Hu, Z., Zhou, L., Zhou, M., 2013. Three-dimensional  
1634 electrochemical process for wastewater treatment: A general review. *Chem. Eng. J.* 228,  
1635 455–467.

- Zhang, C., Zhou, L., Yang, J., Yu, X., Jiang, Y., Zhou, M., 2014. Nanoscale zero-valent iron/AC as heterogeneous Fenton catalysts in three-dimensional electrode system. *Environ. Sci. Pollut. Res.* 21, 8398–8405
- Zhang, Y., Wang, Y., Angelidaki, I., 2015. Alternate switching between microbial fuel cell and microbial electrolysis cell operation as a new method to control H<sub>2</sub>O<sub>2</sub> level in Bioelectro-Fenton system. *J. Power Source.* 291,108-116.
- Zhao, G., Gao, J., Shi, W., Liu, M., Li, D., 2009. Electrochemical incineration of high concentration azo dye wastewater on the in situ activated platinum electrode with sustained microwave radiation. *Chemosphere* 77 (2), 188–193.
- Zhao, X., Liu, S., Huang, Y., 2016. Removing organic contaminants by an electro-Fenton system constructed with graphene cathode. *Toxicol. Environ. Chem.* 98, 530-539
- Zhou, L. Zhou, M., Zhang, C., Jiang, Y., Bi, Z.H., Yang, J., 2013. Electro-Fenton degradation of p-nitrophenol using the anodized graphite felts. *Chem. Eng. J.*, 233, 185-192.
- Zhou, L., Zhou, M., Hu, Z., Bi, Z., Serrano, K.G., 2014. Chemically modified graphite felt as an efficient cathode in electro-Fenton for p-nitrophenol degradation. *Electrochim. Acta* 140, 376-383.
- Zhou, M., Yu, Q., Lei, L., Barton, G., 2007. Electro-Fenton method for the removal of methyl red in an efficient electrochemical system. *Sep. Purif. Technol.* 57 (2), 380–387.
- Zhou, M.H., Liu, L., Jiao, Y. L., Wang, Q., Tan, Q.Q., 2011b. Treatment of high-salinity reverse osmosis concentrate by electrochemical oxidation on BDD and DSA electrodes. *Desalination* 277, 201-206.
- Zhou, M.H., Särkkä H., Sillanpää M.A. 2011a. Comparative experimental study on methyl orange degradation by electrochemical oxidation on BDD and MMO electrodes. *Sep. Purif. Technol.* 78, 290–297.
- Zhu, X., Logan B.E., 2013. Using single-chamber microbial fuel cells as renewable power sources of electro-Fenton reactors for organic pollutant treatment. *J. Hazard. Mater.* 252–253, 198–203.
- Zhu, X., Ni, J., 2009. Simultaneous processes of electricity generation and p-nitrophenol degradation in a microbial fuel cell. *Electrochem. Commun.* 11 (2), 274–277.